haematologica
Journal of the Ferrata Storti Foundation

Fibrin-bound thrombin determines clot structure and blood thrombogenicity in normofibrinogenemia and dysfibrinogenemia

by Siyu Sun, Mark Roest, Rolf T. Urbanus, Elena Campello, Sarah Beck, Cristiana Bulato, Simon D. Connell, Philip G. de Groot, Timea Feller, Dana Huskens, Joke Konings, Rita Marchi, Harmen Middelveld, Patricia Öftering, Bernhard Nieswandt, Alessandro Casini, Robert A. S. Ariëns, Paolo Simioni, Johan W. M. Heemskerk and Bas de Laat

Received: July 1, 2025.
Accepted: January 26, 2026.

Citation: Siyu Sun, Mark Roest, Rolf T. Urbanus, Elena Campello, Sarah Beck, Cristiana Bulato, Simon D. Connell, Philip G. de Groot, Timea Feller, Dana Huskens, Joke Konings, Rita Marchi, Harmen Middelveld, Patricia Öftering, Bernhard Nieswandt, Alessandro Casini, Robert A. S. Ariëns, Paolo Simioni, Johan W. M. Heemskerk and Bas de Laat. Fibrin-bound thrombin determines clot structure and blood thrombogenicity in normofibrinogenemia and dysfibrinogenemia. Haematologica. 2026 Feb 5. doi: 10.3324/haematol.2025.288585 [Epub ahead of print]

Fibrin-bound thrombin determines clot structure and blood thrombogenicity in normofibrinogenemia and dysfibrinogenemia

Siyu Sun[1], Mark Roest[1*], Rolf T. Urbanus[2], Elena Campello[3], Sarah Beck[4], Cristiana Bulato[3], Simon D. Connell[5], Philip G. de Groot[1], Timea Feller[6], Dana Huskens[1], Joke Konings[1], Rita Marchi[7], Harmen Middelveld[1], Patricia Öftering[4], Bernhard Nieswandt[4], Alessandro Casini[7], Robert A. S. Ariëns[6], Paolo Simioni[3], Johan W. M. Heemskerk[1], Bas de Laat[1]

[1] Synapse Research Institute Maastricht, Kon. Emmaplein 7, 6217 KD, Maastricht, The Netherlands; [2]Van Kreveldkliniek, University Medical Centre Utrecht, The Netherlands; [3] Department of Medicine, University of Padua, Padova, Italy; [4]Rudolf Virchow Center for Integrative and Translational Bioimaging & Institute of Experimental Biomedicine, Julius-Maximilians-Universität Würzburg, Germany; [5]Molecular and Nanoscale Physics Group, School of Physics, University of Leeds, Leeds, UK; [6]Discovery and Translational Science Department, Leeds Institute of Cardiovascular and Metabolic Medicine, University of Leeds, Leeds, UK; [7]Division of Angiology and Hemostasis, Department of Medicine, University Hospitals of Geneva, University of Geneva, Switzerland.

*Corresponding authors: Mark Roest Email: M.Roest@thrombin.org, Synapse Research Institute, Kon. Emmaplein 7, 6217 KD, Maastricht, The Netherlands.

Acknowledgement

The authors are grateful to Dr. Jun Wan for his technical assistance with thrombin generation assessments and to Dr. Cuicui Bai for her help with the preparation and purification of PPACK-thrombin.

Sources of funding

This work was supported in part by the China Scholarship Council (CSC, grant number 201906220218 to S.S.).

Authors' disclosures

B.d.L, J.K., D.H., S.S., H.M. and M.R. are employees of the Synapse Research Institute Maastricht (member of the Stago Diagnostic group), P.G.d.G. and J.W.M.H. are advisors of the same institute. The other authors do not report a conflict of interest.

Authors' contributions

S.S., M.R., P.G.d.G., E.C., S.B., P,O. and J.W.M.H. contributed to study design, data interpretation and manuscript writing. S.S., R.T.U., C.B, S.D.C., T.F, D.H, J.K, R.M, H.M. and P.O. contributed to data generation and analysis. E.C., R.M, A.C and P.S. contributed to patient inclusion and clinical data evaluation. R.M, B.N., R.A.S.A., A.C., P.S., P.G.d.G., J.W.M.H. and B.d.L. contributed to material generation, supervision, and manuscript editing.

Materials and Data Availability

Correspondence for material requests should be addressed to Dr. M. Roest. For supplementary material for this paper, see Supplement. All data supporting the present study are provided in the manuscript and the Supplement.

Abstract

In thrombosis and haemostasis, coagulation and platelet activation pathways culminate to form solid fibrin clots, which can become vaso-occlusive or prevent excessive bleeding. We report a novel mechanism describing how developing fibrin clots prolong and modulate the reactivity of thrombin, an enzyme propagating platelet and coagulation activation and forming fibrin from fibrinogen. Using immunological and genetic approaches, we delineate how thrombin bound to the Aα and Bβ chains of fibrin E-domains regulates lateral fibrin fibre extension. Our data reveal that fibrin-bound thrombin remains active and is temporarily protected against inactivation by antithrombin-III. Immunological displacement of thrombin from fibrin profoundly lowered its capacity, whereas a peptide mimicking the Aα-chain binding-site increased its reactivity. In a cohort of patients with congenital dysfibrinogenemia, carrying *FGA*, *FGB* or *FGG* mutations associated with bleeding or thrombosis phenotypes, we noticed a high thrombin capacity and suppressed thrombin-antithrombin-III complex formation, pointing to a prolonged active thrombin lifetime, likely due to abnormal formation of thrombin-containing fibrin. In conclusion, the combination of an impaired clotting and increased thrombogenicity may explain the paradoxical bleeding and thrombotic complications observed in such patients. Development of fibrin-directed agents may offer new therapeutic opportunities to normalize hemostasis or prevent thrombosis.

Keywords

Antithrombin; Clot; Fibrin; Single chain antibody; Thrombin

Introduction

Coagulation operates as a cascade-based process that involves intricate interplays of coagulant and anticoagulant factors in blood plasma as well as platelets, red blood cells and leukocytes, with modulatory actions by endothelial and smooth muscle cells in the vessel wall.[1-3] A key proteolytic enzyme in coagulation is thrombin, which is generated from prothrombin on procoagulant membranes, such as provided by highly activated platelets. Extrinsic thrombin generation is triggered by subendothelial tissue factor (TF), while negatively charged surfaces trigger the process via the intrinsic contact activation pathway.[4] First traces of generated thrombin activate platelets via G-protein coupled receptors, whereas nanomolar levels of thrombin need to be generated to cleave plasma fibrinogen molecules to produce insoluble fibrin meshes or clots.[5,6] The latter proteolytic action of thrombin consists of N-terminal cleavage of fibrinopeptide A (FpA, 16 amino acids) from two fibrinogen Aα–chains, and slower N-terminal cleavage of fibrinopeptide B (FpB, 14 amino acids) from two fibrinogen Bβ-chains.[7,8] A range of heterozygous mutations in the three fibrinogen-encoding genes, *FGA*, *FGB* and *FGG,* associates with dysfibrinogenemia, where carrying subjects can be asymptomatic or in one-third to one-sixth of cases encounter bleeding or thrombotic events.[9] While their haemostatic impairment is usually explained by the quantitative and qualitative fibrinogen defects, underlying causes of the thrombosis risk are not well understood.

The fibrin monomers firstly formed by thrombin consist of so-called D-E-D domains, which then assemble as half-staggered oligomers to polymerize into laterally extending, elastic fibrin fibres.[10,11] In coagulating blood, the result is a stable clot or thrombus, consisting of fibrin matrix and contracting platelets.[12] A crystal structure revealed in 2004 that the E-domain-thrombin complex consists of two thrombin molecules, primarily bound

via the exosite-I and interacting with N-terminal regions of the cleaved Aα- and Bβ- chains.[13] Still unknown is the fate of this medium-affinity thrombin pool. In contrast, well resolved in later studies is the thrombogenic role of high-affinity binding site of thrombin to a splice variant of fibrinogen γ, known as fibrinogen γ-prime (γ').[14]

In the present paper, we employed fibrin-targeted single chain antibodies and fibrin-mimicking peptides as well as advanced biophysical investigations to unravel the reactivity, lifetime and role of the Aα/Bβ–chain fibrin-bound thrombin. We report high levels of this active thrombin pool, which control the process of thrombin generation under conditions of normo- and dysfibrinogenemia. We further provide new evidence for high coagulant activity in patients with congenital dysfibrinogenemia. Unlike the early designations of fibrin as antithrombin-I,[15] we now postulate that fibrin acts as a protective thrombin shield for antithrombin-III capturing.

Methods

A full description of materials, experimental procedures and statistical analysis is provided in the supplement.

Human blood donors

Studies with blood from healthy donors were approved by the Medical Ethical Committee of Maastricht University Medical Centre (NL31480.068.10) and were conducted according to the Declaration of Helsinki. Patient studies were approved by the Research and Ethics Committees of Padua University Hospital Italy (protocol code 4303/AO17, July 28, 2017) and of the University Hospitals of Geneva (Switzerland). Studies were conducted in accordance with the Declaration of Helsinki. Blood donors had not taken anticoagulant or antiplatelet

medication for two weeks and gave written informed consent. Congenital dysfibrinogenemia was classified from reduced fibrinogen activity level in comparison to the antigen level. Genotyping followed the International Society of Thrombosis and Haemostasis classification. Screenings for *FGA*, *FGB* and *FGG* mutations were based on suspected dysfibrinogenemia, and were performed by PCR amplification of fibrinogen coding sequences and Sanger sequencing.[16] For subject cohort testing, plasmas were obtained from 64 healthy individuals (see supplement). Included were samples from 28 males and 36 females, with mean ages of 34 and 32, respectively. Preparation procedures of blood, platelet-rich plasma (PRP) and isolated plasma are described in the supplement.

Thrombin generation and thrombin pool assessments

Thrombin generation measurements were performed within 96-well-plates at 37 °C, employing a low-affinity fluorogenic substrate for thrombin not interfering with the coagulation process, as described for plasma[17] and whole-blood.[18]

To quantify the effect of Nb106 on thrombin activity in TF-triggered plasma over time, we calculated the average thrombin lifetime, defined as the ratio of the total amount of thrombin generated during 60 minutes (endogenous thrombin potential or ETP until the end of the curve, expressed as nM x min) to the amount of prothrombin consumed in this interval. The TF-triggered prothrombin consumption over 60 minutes was measured with a staphylocoagulase assay, as described in the supplement. Calculations of the fibrin-(in)dependent thrombin pools and the average thrombin lifetime are also detailed in the supplement. The term thrombin capacity refers to a plasma coagulation phenotype, distinct from the thrombin generation (TG) curve parameter ETP, as it reflects the overall ability of plasma to generate thrombin in response to a specific trigger rather than the integrated

amount of thrombin formed over time.

Coagulation measurements

Clotting times, clot turbidity and clot contraction measurements as well as fibrinogen function and antigen levels were determined, as described in the supplement.

Advanced microscopy

Atomic force microscopy (AFM) was employed as before for high-resolution imaging of fibrin protofibril and fibril assembly.[19] Multicolour fluorescence and confocal microscopy were used to monitor platelet-dependent coagulation in whole blood under conditions of flow (wall-hear rates 200 and 1000 s^{-1}), as described for mouse blood[20] and human blood.[21]

Thrombin-antithrombin complex assessment

Thrombin-antithrombin (TAT) complex levels were assayed using a high-throughput enzyme-linked immunosorbent assay, employing a novel single chain antithrombin-III antibody Nb1024 (Synapse Research Institute). Similarly, as average thrombin lifetimes, 60-minutes increases in TAT concentrations (nM) were measured in TF-triggered plasmas.

Results

Potent thrombin-suppressive effect of novel single chain antibody

As a novel approach for investigating the interaction between fibrin and thrombin, we used the single chain antibody Nb106. This antibody was obtained from a llama immunized with human fibrin degradation products, and a constructed VHH library. Antibody selection experiments resulted in Nb106, as a single chain antibody that selectively binds to fibrin but

not fibrinogen or thrombin (Suppl. Figure 1A-E). It appeared to require fibrinopeptide B (FpB) cleavage for recognition, indicating that it targets an epitope associated with the Bβ knob–hole interaction. We concluded that Nb106 recognizes a conformationally exposed site on the β-chain of fibrin that becomes available upon FpB release. Further characterization measurements indicated that Nb106 reduced the binding of thrombin to immobilized fibrin layers (Suppl. Figure 1F-G).

Investigating the TF-triggered coagulation process, we observed a profound suppressive effect of Nb106 on maximal thrombin levels and thrombin-cleaving capacity (area-under-the-curve, aka ETP) in platelet-poor plasma, in platelet-rich plasma (PRP) and whole blood (Figure 1A-B). For the thrombin generation process, we observed a dose-dependent inhibition, up to 50% at saturating concentration of 7.5 μM Nb106 (100 μg/mL), *i.e.* far below the normal fibrinogen concentration of 2-4 mg/mL. The indifferent single chain antibody Syn1C6 was ineffective. Although Nb106 caused a major reduction in thrombin level, it did not alter the generation kinetics (Suppl. Figure 2A-B), suggesting interference in a post-acute phase of the clotting process.

To study the contribution of the fibrinogen level, we mixed fibrinogen-depleted plasma and normal plasma in various ratios, and re-assessed the TF-triggered coagulation process. Without fibrinogen, relatively low amounts of thrombin were formed that were not sensitive to Nb106 (150 μg/mL). At higher fibrinogen concentrations, both the thrombin level and the suppression by Nb106 increased (Figure 1C). Addition of γ'-enriched fibrinogen to normal plasma resulted in a reduced Nb106 effect, compared to normal fibrinogen (Figure 1D-E). This suggested that Nb106 did not interfere with the high-affinity binding site for thrombin in fibrinogen-γ'.[14] When Nb106 was spiked into normal plasma at later time points, the inhibitory effect disappeared after 5-10 minutes of TF triggering (Suppl. Figure 2C-D).

Hence the time slot of suppression coincided with the buildup of the fibrin clot.

To assess the reliance on coagulation factors, we studied thrombin generation in several coagulation factor-deficient plasmas. We observed that Nb106 caused major reductions in thrombin formation in normal pool plasma (NPP) and in plasmas deficient in coagulation factors IX, XI or XII (Figure 2A-D). In contrast, it was ineffective in the absence of fibrinogen or antithrombin-III (Figure 2E-F), as quantified from measured thrombin maxima and thrombin capacity levels (Figure 2G). This requirement of fibrinogen and antithrombin was also retained in the presence of platelets (Suppl. Figure 3A-G). As expected, at antithrombin-III deficiency, higher thrombin levels were reached, with maxima raising from 150 to 450 nM (Figure 2F), due to the impaired inactivation of proteolytically active thrombin.

To determine whether the fibrinogen dependence was pertained upon triggering of the intrinsic pathway, we measured the kaolin-induced thrombin generation. Similar to the TF-triggered condition, Nb106 reduced the thrombin capacity by 57.39 ± 21.79 % in NPP, but not in fibrinogen-deficient plasma (Suppl. Figure 4A-C).

Assessment of the fibrin-bound pool of active thrombin attacked by Nb106

From the results so far, we hypothesized that the Nb106 displaces thrombin from growing fibrin fibres, thereby rendering it susceptible to inhibition by antithrombin-III through TAT complex formation. To check this, we measured average thrombin lifetimes in both normal and antithrombin-deficient plasma, i.e. by comparing the thrombin capacity (ETP, nM x min) and the prothrombin consumption (nM) after 60-minutes of TF triggering (Figure 2H-I). Herein, we distinguished between a fibrin-independent thrombin pool 1 (thrombin capacity resistant to Nb106), and a fibrin-dependent thrombin pool 2 for the remaining capacity

(Figure 2J). Using NPP, average thrombin lifetimes for pool 1 and 2 were obtained of 1.21±0.13 and 2.70±0.45 minutes, respectively (means ± SD, n=5). For antithrombin-deficient plasma (no Nb106 effect) this lifetime was prolonged to 11.98±0.17 minutes (Figure 2K). These values are in line with literature where thrombin was spiked into antithrombin-deficient plasmas.[22] Hence, we concluded that that the fibrin-binding Nb106 shortened the average thrombin lifetime by 2.2-fold, whereas the absence of antithrombin-III prolonged this lifetime by 9.9-fold.

Initial light transmission microscopy indicated that Nb106, in both TF-triggered NPP and antithrombin-deficient plasma, made the fibrin fibre network less compact (Figure 2L). Fibrin fibres also appeared thicker without antithrombin-III. This suggested that, in normal plasma, the fibrin-bound (Nb106-replacable) pool of thrombin has a critical role in fibrin network formation.

Considering prior evidence of a thrombin binding site in N-terminal regions of fibrin Aα and Bβ chains,[13] we assessed how Nb106 acted in plasmas pretreated with specific fibrinogen-cleaving proteases. Plasma incubation with protease III from the snake *Crotalus atrox*, which N-terminally cleaves fibrinogen Bβ-chains,[23,24] halved the thrombin generation and importantly annulled the inhibition by Nb106 (Suppl. Figure 5A). Plasma treatment with ancrod from *Calloselasma rhodostoma*, which C-terminally cleaves fibrinogen Aα-chains[25], was however ineffective on coagulation in the presence or absence of Nb106 (Suppl. Figure 5B). Addition of the fibrin polymerization-inhibiting peptide GPRP[26] reduced thrombin generation by 20%, but did not alter the suppression by Nb106 (Suppl. Figure 5C).

We then checked for effects with clinically relevant anticoagulants, using the reversible thrombin inhibitor dabigatran or activated protein C. Although either intervention suppressed thrombin generation as expected, both left the extent of Nb106 inhibition

unchanged (Suppl. Figure 5D-E). To substantiate the idea that Nb106 displaces thrombin from growing fibrin fibres, we first examined the effects of the irreversible thrombin inhibitor PPACK. This treatment caused a concentration-dependent delay and reduction in thrombin generation, whereas the inhibitory effect of Nb106 remained unchanged (Suppl. Figure 7A). Second, we made a purified preparation of PPACK-inactivated thrombin, blocking its active site but retaining the exosites (Suppl. Figure 6). Strikingly, the addition of PPACK-thrombin to NPP suppressed the thrombin generation to the same extent as Nb106 (Suppl. Figure 7B). In contrast, the PPACK-thrombin was without effect in fibrinogen-deficient plasma (Suppl. Figure 7C). These results suggested that both NB106 and PPACK-thrombin compete with active thrombin for binding sites on fibrin, and thereby promote inactivation of the released thrombin by antithrombin-III. Additionally, these findings provide an indication that the Nb106 binding site in fibrin locates near the N-terminal Bβ chain in the D-E-D domain, *i.e.* a known fibrin knob-allocated position of thrombin.[13] We hence concluded that displacement of thrombin in the E domain can relieve its protection to antithrombin-III inactivation.

Inter-subject variability of thrombin generation not affected by Nb106

To assess for inter-subject differences, we also assessed the TF-triggered coagulation in plasmas from 64 healthy subjects, applying a near maximal inhibiting Nb106 concentration of 150 µg/mL. Across all subjects, Nb106 did not alter thrombin lag times, while it consistently reduced thrombin maxima and thrombin capacity levels by 53±11% and 55±12% (mean±SD, n=64, $p<0.05$), respectively (Suppl. Figure 8A-B). Interestingly, when plotted against the fibrinogen activity level (Claus method), we noticed an increased capacity, which was corrected by the Nb106 up to 4 g/L fibrinogen. This demonstrated a consistent

downregulation of thrombin generation by the antibody. However, thrombin capacities with and without Nb106 were strongly correlated (R^2=0.66, p<0.0001) (Suppl. Figure 8D). Across plasmas, the extent of thrombin capacity inhibition by Nb106 showed a statistically significant but modest correlation (R^2=0.15, p=0.0019) (Suppl. Figure 8C), in support of crucial roles of other coagulation factors in the thrombin generation process.[27,28]

Displacement of thrombin from fibrin altering fibrin fibre structure and function

Considering the potent antithrombin effect of Nb106, we next examined how it affected fibrin protofibril formation and polymerisation. In measurements of mechanically stirred clotting times, plasma triggering with 1-1000 pM TF was not affected by Nb106 (Figure 3A). In contrast, in light disturbance measurements, Nb106 essentially annulled the TF-induced optical density changes (Figure 3B). This suggested that the clots formed with Nb106 are light transparent, which idea was also supported by confocal microscopy, showing fibrin microclots not extending to fibrin fibres (Suppl. Figure 9A). Additional clot lysis experiments showed that the the loose transparent clots formed with Nb106 were still susceptible to tPA-induced lysis, although the minimal turbidity changes preclude reliable determination of the lysis time (Suppl. Figure 9B).

Fibrin fibre formation proceeds by polymerization of fibrin monomers into protofibrils.[19] For higher-resolution examination, we applied atomic force microscopy allowing visualization of the protofibril formation on a molecular scale. Using mixtures of fibrinogen and thrombin, we observed that the Nb106 within 1 minute enhanced and retained the formation of protofibril molecules (Figure 3C-D). This effect is compatible with thrombin displacement from the central D-E-D regions, which results in more soluble thrombin to induce additional fibrinogen cleavages. Longer-time images showed that Nb106

blocked normal extension of fibrin fibres, leaving shorter and thinner protofibril structures (Figure 3E). These profound structural changes prompted us to examine Nb106 effects on the physiological and biophysical properties of formed clots under conditions of dysfibrinogenemia.

Altered thrombin generation and fibrin clots in patients with congenital dysfibrinogenemia

Patients with congenital dysfibrinogenemia exhibit functional alterations in fibrinogen, which are asymptomatic or associate with bleeding or thrombotic events.[29] Multiple pathogenic mutations have been identified, in part dominant, which concentrate in distinct regions of the *FGA*, *FGB* and *FGG* genes.[9,30] To examine the thrombin-fibrin interactions in dysfibrinogenemia, we studied plasmas from 21 patients with a mutation in *FGA* (n=12), *FGB* (n=4) or *FGG* (n=5). Given the rarity of this disorder, this cohort represents one of the largest collections of patients with fibrinogen gene mutations.

All patients presented with a low fibrinogen function (assessed by the Claus method) relative to the fibrinogen antigen level, while 11 patients had sub-normal antigen levels as well (Table 1). Across mutations, 9 patients had experienced minor bleeding symptoms, 2 had thrombotic events, while for three mutations (9 additional patients) incidental bleeding and thrombosis has been documented (Table 1). With all patients showing lower fibrinogen function than antigen levels, they were analyzed as a single group, despite the heterogeneity in mutation type and gene and clinical penetrance.

Coagulation analysis indicated that in plasmas from 13 out of 21 patients, across all three genes, thrombin generation exceeded the reference values assessed for healthy subjects, while only 3 plasmas showed low maximal thrombin levels (<150 nM) (Table 1). Addition of Nb106 suppressed both the maximal and capacity levels, whilst values remained

supranormal in 11-14 patients (Figure 4A-F). Lowest suppression of <40% was observed in the 6 patients with sub-normal functional fibrinogen, *i.e.* 0.77±0.43 g/L (mean ± SD). When plotted against the fibrinogen function level, the patient group as a whole scored high in thrombin generation (Figure 4G). This could be considered as clinically relevant, since already small increases in thrombin generation profiles have been associated with thrombogenic abnormalities.[31,32] Six of the patients (3x *FGA*, 2x *FGB*, 1x *FGG* mutations) with high thrombin generation had experienced bleeding symptoms (Table 1).

In the patient group, TF-triggered clot retraction in the presence of platelets was high given taking into account their low fibrinogen values(Figure 4H), but this was not the case for plasma turbidity changes (Figure 4I). Together, this suggested an enhanced activity of fibrin-bound (antithrombin-resistant) thrombin, yet showing high contractility, in at least part of the patient plasmas. To further assess this, we measured the complex formation of thrombin-antithrombin (TAT) in activated plasma samples from controls and patients, using a new single chain antibody Nb1024. Since TAT levels reflect prothrombin consumption when combined with thrombin capacity values, these were also used to calculate average thrombin lifetimes. Markedly, we observed significantly lower TAT levels in the total patient group, when compared to the controls, which translated into prolonged thrombin lifetimes for half of the patients (Figure 4J-K). These results jointly show that, in at least part of the studied dysfibrinogenemia patients, across gene mutations, the altered fibrinogen function is accompanied by a prolonged activity of fibrin-bound thrombin. The combination of loss-of-function (low or dysfunctional fibrinogen) and gain-of-function (enhanced thrombin activity) may underlie the paradoxical coexistence of hemostasis and thrombotic complications regularly observed in these patients.

Thrombin-fibrin interactions affecting thrombus formation at low shear rate

Alignment of the N-terminal regions of fibrinogen Aα-and Bβ-chains showed high amino acid sequence similarly between human and mouse, in particular around the thrombin cleavage site and the adjacent thrombin exosite-I binding domain (Suppl. Figure 10A-D). The inter-species conservation prompted us to also evaluate the effects of Nb106 in mouse blood. Similar as in the human system, in plasmas from C57BL/6 mice the antibody about halved the maximal thrombin and thrombin capacity levels (Figure 6A), while it similarly distorted the formation of laterally extending fibrin fibres, changing these into amorphous structures (Figure 6B).

As a proxy measurement for thrombus formation in vivo, we used a microfluidic approach, in which recalcified whole blood in the presence of TF was flowed over collagen.[21] In this ex vivo system, addition of Nb106 (100 μg/mL) led to a significantly reduced and delayed fibrin fibre formation, but unchanged platelet-related thrombus characteristics, upon perfusion of the blood at low, venous wall-shear rate of 200 s^{-1} (Figure 6C-F). On the other hand, upon flow at high arterial shear rate (1000 s^{-1}), fibrin formation and platelet deposition remained unaltered with Nb106 (Suppl. Figure 11). Similarly observations were made with human blood (Suppl. Figure 12). These data point to an overall anticoagulant effect of Nb106 especially under circumstances of stasis or low shear.

Procoagulant effect of fibrin regions interacting with thrombin via exosite I

To further proof the concluded interaction of thrombin with fibrin Aα and/or Bβ N-terminal regions, we synthesized peptides corresponding to the conserved exosite-I binding sites in these regions, *i.e.* Pep1 consisting of residues 40-69 of fibrinogen-α, and Pep2 composed of residues 71-105 of fibrinogen-β (Suppl. Figure 10). When tested at 0 and 500 μM, Pep1 but

not Pep2 showed a strong but temporary enhancing effect in TF-triggered thrombin generation at >100 μM, *i.e.* 5 times higher than the bivalent concentration of fibrinogen in normal plasma (Figure 5A). We further found that Pep1 was similarly effective in fibrinogen-depleted and antithrombin-depleted plasma. In all cases, it caused a transient enhancement in thrombin levels, regardless of the slower decay in the absence of antithrombin-III (Figure 5A-F). In addition, Pep1 but not Pep2 shortened TF-triggered turbidity changes in plasma (Figure 5G-H) and prolonged the clot lysis time (Suppl. Figure 9C), but it did not appreciably affect fibrin network formation (Figure 5I). Pep1 furthermore reduced the inhibiting effect of Nb106 (Figure 5J-K). Taken together, this suggested that also Pep1, as thrombin exosite-I binding peptide derived from the fibrin Aα N-terminal region, ▯ likely in equilibrium with the corresponding sequence in fibrin ▯ temporarity protected thrombin for inactivation by antithrombin-III.

To confirm this, we tested aptamers directed against thrombin exosite-I (Apt1), exosite-II (Apt2), or both (Apt3). We found that Apt1 and Apt2 similarly enhanced thrombin generation but now leaving the inhibiting effect of Nb106 unaffected (Suppl. Figure 13). In contrast, Apt3 fully blocked the process, i.e. by effectively annulling thrombin activity (Suppl. Figure 13D,H). These results jointly indicate that interference in the binding of thrombin to antithrombin-III enhances its cleavage capacity.

Discussion

Our study reveals the key importance of N-terminal regions in the fibrin Aα- and Bβ-chains regarding binding and retaining proteolytically active thrombin to allow lateral extension of fibrin fibres. Mechanistically, we show that this binding provides temporal protection against inactivation by antithrombin-III. This insight and the various tools developed in our study can

provide novel approaches to rebalance the fibrin clotting process in (venous) thrombosis and impaired haemostasis.

Insight into the role of thrombin-bound fibrin came from the use of a novel single chain antibody Nb106, raised against fibrin degradation products and characterized as binding to fibrin D-E-D regions, but not to full length fibrinogen. In TF-triggered plasma or blood, Nb106 abrogated half of the thrombin cleavage capacity, which effect relied on the presence of both fibrinogen and antithrombin-III. Supported by experiments using PPACK-thrombin, our data indicated that Nb106 released thrombin from growing fibrin fibres, thereby enhancing its inactivation by antithrombin-III. As the Nb106 effect disappeared after fibrinogen treatment with protease III, we considered that the binding site is at or close to the N-terminal region of fibrin Bβ. Conversely, the peptide Pep1 corresponding to the N-terminal Aα chain increased the thrombin activity, similarly as thrombin exosite-I binding aptamers, which region according to crystallographic evidence locates close to the N-terminal Bβ chain. This scheme agrees with the known structure of two thrombin molecules bound to central E-domain of fibrin via exosite-I recognition sites in the Aα and Bβ chains (Figure 7A-D).

Our findings are also in agreement with the early, 1997, identification of low affinity thrombin binding sites on fibrin, which were then provisionally assigned to the N-terminal Aα chains and Bβ chains, *i.e.* adjacent to the thrombin cleavage sites producing FpA and FpB, respectively. Of note, there is evidence that similar sites are also involved in fibrin monomer polymerization,[23,36] suggesting that also fibrin monomer competition dislodges thrombin from growing fibres, and thereby re-exposes its active site for clot extension.[34] Our measurements of thrombin activity and prothrombin consumption made us conclude that the binding to fibrin led to a 2.2-fold increase in average lifetime, which is less than the 10-

fold increase observed in the absence of antithrombin-III.

We furthermore observed that the thrombin binding was required for lateral growth of fibrin monomers to form the network of fibrin fibres. The abrogation of optical density changes in clotting plasma with Nb106, despite unaltered clotting times, could be explained by the formation of transparent, essentially non-fibrillar clots in the presence of Nb106. Also other authors have observed that the formation of a thin fibrin network causes minimal changed in light scattering.[37] Our atomic force microscopy experiments also demonstrated that Nb106 stimulated the formation of thin and amorphous protofibrils instead of mature fibrin fibres. Jointly, our data point to the presence of a substantial pool of proteolytically active thrombin that binds to fibrin, is protected from anticoagulation, and is required for elastic fibrin clot formation.

To further substantiate the findings, we defined and quantified two similarly sized thrombin pools: a fibrin-dependent (Nb106-sensitive) pool, corresponding to the fraction of thrombin capacity suppressed by Nb106, and a fibrin-independent (Nb106-insensitive) pool, corresponding to the remaining capacity unaffected by the antibody. This approach supported the view that fibrin serves as a dynamic reservoir maintaining thrombin activity at the clot interface. Mechanistically, as stipulated for other natural thrombin inhibitors,[38] our data demonstrate that fibrin acts as a potent redirector of thrombin's targets in coagulation. In analogy, endothelial-expressed thrombomodulin redirects thrombin's targets towards protein C activation.[39] The unravelled prolonged binding of thrombin to fibrin further explains earlier *in vivo* observations on thrombotic venules and arterioles in mouse, showing consistent co-localization of labelled (pro)thrombin with formed fibrin clots.[40]

Patients with congenital dysfibrinogenemia carrying variety of mutations in the fibrinogen genes *FGA*, *FGB* or *FGG*, present with heterozygous symptoms, where a mild

bleeding phenotype is more frequently observed than thrombophilia.[9,41] This is also seen in the 21 patients included in the present study, with half of the subjects showing mostly mild bleeding symptoms and 2 presenting with thrombotic complications. Intriguingly, the majority of 13 patients showed higher than normal thrombin generation levels, which were partly normalized by Nb106, whereas only 3 patients had relatively low levels. It should be mentioned here that the molecular relation between the usually heterozygous mutations and the phenotype is complex, because of the presence of heterodimeric fibrinogen molecules.[9]

In the patient group, we furthermore noted a lower than normal TAT complex formation. Comparison of the thrombin generation profile and the TAT formation pointed to a prolonged average thrombin lifetime in the whole patient group. This hence suggests a prolonged retainment of thrombin at the fibrin network, which is in line with the often altered (porous, lace-like, thick fibre) fibrin networks observed in dysfibrinogenemia.[42] Our data with 21 patients however will need to be followed up by more detailed studies to establish the precise relation between a prolonged thrombin activity and a risk of thrombophilia, considering that the overall low fibrinogen antigen levels can also result in bleeding phenotype. Our hypothesis with respect to severe dysfibrinogenemia is that an imperfect alignment of the fibrin Aα and Bβ chains keeps thrombin connected to the growing fibrin fibres, temporarily preventing its inactivation by antithrombin-III (Figure 7E). This idea was further supported by the increased thrombin activity observed by Pep1 corresponding to the N-terminal Aα chain. In this respect, fibrin as a previously assigned antithrombin-I, differs from antithrombin-III in that it keeps thrombin active in the proteolytic cleavage of substrates like fibrinogen molecules.

In conclusion, thrombin binding to fibrin, displaced by Nb106 and altered in cases of

dysfibrinogenemia, regulates not only lateral fibrillar extension, but also provides protection against antithrombin-III inactivation. Constructs of Nb106 and fibrin Aα/Bβ-derived peptides may provide novel anti- and procoagulant treatment options for thrombosis and haemostasis, respectively.

References

1. Macfarlane RG. An enzyme cascade in the blood clotting mechanism, and its function as a biochemical amplifier. Nature. 1964;202:498-499.
2. Hoffman M, Monroe DM. A cell-based model of hemostasis. Thromb Haemost. 2001;85(6):958-965.
3. Furie B, Furie BC. Mechanisms of thrombus formation. N Engl J Med. 2008;359(9):938-949.
4. Mann KG, Brummel K, Butenas S. What is all that thrombin for? J Thromb Haemost. 2003;1(7):1504-1514.
5. Versteeg HH, Heemskerk JW, Levi M, Reitsma PH. New fundamentals in hemostasis. Physiol Rev. 2013;93(1):327-358.
6. Sang Y, Roest M, de Laat B, de Groot PG, Huskens D. Interplay between platelets and coagulation. Blood Rev. 2021;46(1):100733.
7. Hantgan RR, Simpson-Haidaris PJ, Francis CW, Marder VJ. Fibrinogen structure and physiology. In: Colman RW, Clowes AW, George JN, Goldhaber SZ, Marder VJ, editors. Hemostasis and thrombosis: basic principles and clinical practice. Philadelphia (PA): Lippincott Williams & Wilkins; 2001. p. 203-232.
8. Soya K, Terasawa F, Okumura N. Fibrinopeptide A release is necessary for effective B:b interactions in polymerisation of variant fibrinogens with impaired A:a interactions. Thromb Haemost. 2013;109(2):221-228.
9. McDonagh J. Dysfibrinogenemia and other disorders of fibrinogen structure and function. In: Colman RW, Clowes AW, George JN, Goldhaber SZ, Marder VJ, editors. Hemostasis and thrombosis: basic principles and clinical practice. Philadelphia (PA): Lippincott Williams & Wilkins; 2001. p. 855-892.
10. Mosesson MW. Fibrinogen and fibrin structure and functions. J Thromb Haemost. 2005;3(8):1894-1904.
11. Weisel JW, Litvinov RI. Mechanisms of fibrin polymerization and clinical implications. Blood. 2013;121(10):1712-1719.
12. Wolberg AS, Sang Y. Fibrinogen and factor XIII in venous thrombosis and thrombus stability. Arterioscler Thromb Vasc Biol. 2022;42(8):931-941.

13. Pechik I, Madrazo J, Mosesson MW, Hernandez I, Gilliland GL, Medved L. Crystal structure of the complex between thrombin and the central E region of fibrin. Proc Natl Acad Sci U S A. 2004;101(9):2718-2723.
14. Macrae FL, Swieringa F, Heemskerk JW, Ariëns RA. High fibrinogen γ' levels in patient plasma increase clot formation at arterial and venous shear rate. Blood Adv. 2021;5(17):3468-3477.
15. Smith GF. Fibrinogen-fibrin conversion. The mechanism of fibrin-polymer formation in solution. Biochem J. 1980;185(1):1-11.
16. Marchi R, Neerman-Arbez M, Gay V, et al. Comparison of different activators of coagulation by turbidity analysis of hereditary dysfibrinogenemia and controls. Blood Coagul Fibrinolysis. 2021;32(2):108-114.
17. Vanschoonbeek K, Feijge MA, van Kampen RJ, et al. Initiating and potentiating role of platelets in tissue factor-induced thrombin generation in the presence of plasma: subject-dependent variation in thrombogram characteristics. J Thromb Haemost. 2004;2(3):476-484.
18. Sun S, Campello E, Zou J, et al. Crucial roles of red blood cells and platelets in whole blood thrombin generation. Blood Adv. 2023;7(21):6717-6731.
19. Allan P, Uitte de Willige S, Abou-Saleh RH, Connell SD, Ariëns RA. Evidence that fibrinogen γ' directly interferes with protofibril growth: implications for fibrin structure and clot stiffness. J Thromb Haemost. 2012;10(6):1072-1080.
20. Beck S, Öftering P, Li R, et al. Platelet glycoprotein V spatio-temporally controls fibrin formation. Nat Cardiovasc Res. 2023;2(4):368-382.
21. Brouns S, van Geffen JP, Campello E, et al. Platelet-primed interactions of coagulation and anticoagulation pathways in flow-dependent thrombus formation. Sci Rep. 2020;10(1):11910.
22. Rühl H, Müller J, Harbrecht U, et al. Thrombin inhibition profiles in healthy individuals and thrombophilic patients. Thromb Haemost. 2012;107(5):848-853.
23. Pandya BV, Gabriel JL, O'Brien J, Budzynski AZ. Polymerization site in the beta chain of fibrin: mapping of the B beta 1-55 sequence. Biochemistry. 1991;30(1):162-168.
24. Moskowitz KA, Budzynski AZ. The (DD)E complex is maintained by a composite fibrin polymerization site. Biochemistry. 1994;33(42):12937-12944.

25. McDonagh RP, Carrell NA, Roberts HR, Blatt PM, McDonagh J. Fibrinogen Chapel Hill: hypodysfibrinogenemia with a tertiary polymerization defect. Am J Hematol. 1980;9(1):23-38.
26. Crossen J, Diamond SL. Thermal shift assay to probe melting of thrombin, fibrinogen, fibrin monomer, and fibrin: Gly-Pro-Arg-Pro induces a fibrin monomer-like state in fibrinogen. Biochim Biophys Acta Gen Subj. 2021;1865(2):129805.
27. Bai C, Konings J, Ninivaggi M, Lancé M, de Laat B, de Laat-Kremers R. Assessing the individual roles of FII, FV, and FX activity in the thrombin generation process. Front Cardiovasc Med. 2022;9:1000812.
28. Stobb MT, Neeves KB, Monroe DM, Sindi SS, Leiderman K, Fogelson AL. Mathematical modeling identifies clotting factor combinations that modify thrombin generation in normal and factor VIII-, IX-, or XI-deficient blood. Res Pract Thromb Haemost. 2024;8(7):102570.
29. Casini A, Moerloose P, Neerman-Arbez M. Clinical, laboratory, and molecular aspects of congenital fibrinogen disorders. Semin Thromb Hemost. 2025;51(2):103-110.
30. De Moerloose P, Casini A, Neerman-Arbez M. Congenital fibrinogen disorders: an update. Semin Thromb Hemost. 2013;39(6):585-595.
31. Zanetto A, Campello E, Bulato C, et al. Impaired whole blood thrombin generation is associated with procedure-related bleeding in acutely decompensated cirrhosis. J Hepatol. 2025;82(6):1023-1035.
32. Spiegelenberg JP, de Laat-Kremers R, Roest M, et al. Low thrombin inactivation capacity is associated with an increased risk of recurrent ischemic events after ischemic stroke at a young age. J Thromb Haemost. 2025;23(3):978-988.
33. Hsieh KH. Localization of an effective fibrin beta-chain polymerization site: implications for the polymerization mechanism. Biochemistry. 1997;36(31):9381-9387.
34. Hsieh K. Thrombin interaction with fibrin polymerization sites. Thromb Res. 1997;86(4):301-316.
35. Becker DL, Fredenburgh JC, Stafford AR, Weitz JI. Exosites 1 and 2 are essential for protection of fibrin-bound thrombin from heparin-catalyzed inhibition by antithrombin and heparin cofactor II. J Biol Chem. 1999;274(10):6226-6233.

36. Siebenlist KR, DiOrio JP, Budzynski AZ, Mosesson MW. The polymerization and thrombin-binding properties of des-(B beta 1-42)-fibrin. J Biol Chem. 1990;265(30):18650-18655.
37. Wolberg AS, Campbell RA. Thrombin generation, fibrin clot formation and hemostasis. Transfus Apher Sci. 2008;38(1):15-23.
38. Huntington JA. Natural inhibitors of thrombin. Thromb Haemost. 2014;111(4):583-589.
39. Marar TT, Matzko CN, Wu J, et al. Thrombin spatial distribution determines protein C activation during hemostasis and thrombosis. Blood. 2022;139(12):1892-1902.
40. Berny MA, Munnix IC, Auger JM, et al. Spatial distribution of factor Xa, thrombin, and fibrin(ogen) on thrombi at venous shear. PLoS One. 2010;5(3):e10415.
41. Casini A, de Moerloose P. How I treat dysfibrinogenemia. Blood. 2021;138(21):2021-2030.
42. Sugo T, Endo H, Matsuda M, et al. A classification of the fibrin network structures formed from the hereditary dysfibrinogens. J Thromb Haemost. 2006;4(8):1738-1746.
43. Marchi R, Vilar R, Durual S, et al. Fibrin clot properties to assess the bleeding phenotype in unrelated patients with hypodysfibrinogenemia due to novel fibrinogen mutations. Thromb Res. 2021;197(1):56-64.
44. Köhler S, Schmid F, Settanni G. The internal dynamics of fibrinogen and its implications for coagulation and adsorption. PLoS Comp Biol. 2015;11(7):e1004346.

Table 1. Characteristics of plasmas from patients with congenital dysfibrinogenemia. Shown are genetic variants and levels of fibrinogen antigen and function (Claus methods). Reference values for fibrinogen antigen were 2.4-3.6 g/L, for fibrinogen function 1.5-4.5 g/L; and for thrombin generation maxima 80-254 nM. Information on mutation-linked phenotypes came from Ref.[9] and ClinVar Febr. 2025 (https://www.ncbi.nlm.nih.gov/clinvar/). Patients were included, based on studies described before.[16,43]

Patient	Genetic variant	Sex	Age	Patient phenotype	Mutation-linked phenotype in literature	Fibrinogen antigen (g/L)	Fibrinogen function (g/L)	Thrombin maximum (nM)
FGA1	*FGA* c.95 G>A (p.Gly32Glu) het	M	28	(prolonged PT)	(likely pathogenic)	2.64	**1.06**[*]	**678**[#]
FGA2	*FGA* c.95 G>A (p.Gly32Glu) het	M	62	epistaxis in childhood	(likely pathogenic)	3.03	**1.08**[*]	**504**[#]
FGA3	*FGA* c.112 A>G (p.Arg38Gly) het	M	53	(prolonged PT)	reported bleeding and thrombosis, polymer region	3.03	**0.65**[*]	**328**[#]
FGA4	*FGA* c.149 C>G (p.Ser50*) hom	F	61	cranial bleeding, aortic thrombosis	novel (n.d.)	**1.30**[*]	**0.35**[*]	**320**[#]
FGA5	*FGA* c.112 A>G (p.Arg38Gly) het, *FGB* c.794 C>T (p.Pro265Leu) het	F	63	family study	reported bleeding and thrombosis, polymer region (FGA)	3.18	**1.04**[*]	202
FGA6	*FGA* c.112 A>G (p.Arg38Gly) het	F	22	prior bleeding	reported bleeding and thrombosis, polymer region	2.40	**0.58**[*]	**297**[#]
FGA7	*FGA* c.104 G>A (p.Arg35His) het	M	23	asymptomatic	reported bleeding and thrombosis (pathogenic)	3.17	**1.40**[*]	174
FGA8	*FGA* c.104 G>A (p.Arg35His) het	F	39	mild bleeding	reported bleeding and thrombosis (pathogenic)	2.70	**1.30**[*]	236
FGA9	*FGA* c.104 G>A (p.Arg35His) het	F	38	mild bleeding	reported bleeding and thrombosis (pathogenic)	3.26	**1.40**[*]	**387**[#]
FGA10	*FGA* c.104 G>A (p.Arg35His) het	F	27	mild bleeding	reported bleeding and thrombosis (pathogenic)	**2.19**[*]	**1.10**[*]	158
FGA11	*FGA* c.104 G>A (p.Arg35His) het	M	39	asymptomatic	reported bleeding and thrombosis (pathogenic)	3.54	1.50	233
FGA12	*FGA* c.104 G>A (p.Arg35His) het	F	22	asymptomatic	reported bleeding and thrombosis (pathogenic)	**2.18**[*]	**0.60**[*]	**275**[#]
FGB1	*FGB* c.886 T>C (p.Trp296Arg) hom	M	5	prior bleeding	novel (n.d.)	**1.11**[*]	**0.68**[*]	**329**[#]
FGB2	*FGB* c.886 T>C (p.Trp296Arg) het	M	38	bleeding after minor injuries	novel (n.d.)	**1.38**[*]	**1.06**[*]	**531**[#]
FGB3	*FGB* c.886 T>C (p.Trp296Arg) het	F	26	family study	novel (n.d.)	**1.71**[*]	**1.09**[*]	**559**[#]
FGB4	*FGB* c.534 G>C (p.Lys178Asn) het	M	28	family study	novel (n.d.)	**1.98**[*]	1.61	141
FGG1	*FGG* c.998 A>G (p.His333Arg) het	M	44	thrombosis of superior mesenteric vein	novel (n.d.)	**0.84**[*]	**0.42**[*]	**386**[#]
FGG2	*FGG* c.998 A>G (p.His333Arg) het	F	13	prior bleeding	novel (n.d.)	**1.14**[*]	**0.91**[*]	**271**[#]
FGG3	*FGG* c.1223 C>T (p.Thr408Ile) het	M	24	(prolonged PT)	novel (n.d.)	**0.87**[*]	**0.85**[*]	**276**[#]
FGG4	*FGG* c.323 C>G (p.Ala108Gly) het	M	41	prior bleeding	reported bleeding (likely pathogenic)	**1.74**[*]	1.60	114
FGG5	*FGG* c.1007 T>C (p.Met336Thr) het	F	27	menorrhagia (prolonged PT)	fibrinogen Asahi (pathogenic)	4.26	**0.35**[*]	99
Reference values						2.4-3.6	1.5-4.5	80-254

*Bold values are outside normal ranges. Values below are marked with *, and those above are marked with #.

Legends to figures

Figure 1. Major anticoagulant effect of fibrin-directed single chain antibody Nb106.

(**A-B**) Samples of plasma, platelet-rich plasma (PRP) and whole blood were pre-incubated with vehicle control solution, anti-fibrin single chain antibody Nb106 (25-100 µg/mL) or indifferent single chain antibody Syn1C9 (100 µg/mL). Coagulation was triggered with 1 pM TF, phospholipids and $CaCl_2$/$MgCl_2$; see methods. (**A**) Representative thrombin generation curves with autologous plasma (**i**), PRP (**ii**) and whole blood (**iii**). (**B**) Quantified thrombin cleavage capacity (endogenous thrombin potential, ETP), relative to the control condition. Means ± SD (n=3 experiments). Statistically significant p values are shown in the figure (one-way ANOVA, non-parametric). Other parameters indicated in Suppl. Figure 2. (**C-D**) Effect of Nb106 in dependency of fibrinogen concentration. (**C**) Normal pool plasma (NPP, 2.90 g/L fibrinogen) was mixed with fibrinogen-deficient plasma at different volume ratios, and thrombin generation was measured in the presence of 0-150 µg/mL Nb106. Representative thrombin generation is shown (**i-iii**). (**D**) NPP was supplemented with fibrinogen-γ or fibrinogen-γ′ (1.2 g/L) and thrombin generation was measured in the presence of of 0-150 µg/mL Nb106. Representative curves given (**i-iii**). (**E i**)-Heatmap of normalized thrombin capacity for condition of panel C; (**E ii**) similar heatmap for condition of panel D. Means ± SD (n=3). 100% represents condition without fibrinogen and Nb106.

Figure 2. Anticoagulant effect of Nb106 relying on both fibrinogen and antithrombin.

(**A-G**) TF-triggered thrombin generation was measured in different plasma types containing vehicle control solution or Nb106 (100 µg/mL), as in Figure 1. Compared were normal pool plasma (NPP) (**A**), and plasmas deficient in factor IX (**B**), factor XI (**C**), factor XII (**D**), fibrinogen

(**E**), or antithrombin (**F**). Generation of thrombin over time (n=3) and process quantification with statistics (**G**). (**H-K**) Assessment of fibrin-independent and -dependent thrombin pools 1 and 2 in coagulating plasma. NPP and antithrombin-deficient plasma (ATDP) were activated as above, and thrombin capacity (ETP) measured over 60 minutes (**H**). Prothrombin consumption over 60 minutes assessed in activated subsamples (**I**). Fractions (**J**) and lifetimes (**K**) of thrombin pool 1 (Nb106-insensitive, fibrin-independent in NPP) and pool 2 (Nb106-sensitive, fibrin-dependent in NPP) were calculated, as in the methods section. Means ± SD (n=3-5), two-way ANOVA, non-parametric. (**L**) Fibrin fibre structures formed in normal pool plasma (NPP) and antithrombin-deficient plasma. Human NPP and antithrombin-III-deficient plasma (ATDP) was triggered with TF, procoagulant phospholipids and Ca^{2+}. Plasma samples were preincubated with vehicle control medium or Nb106 (100 µg/mL). Shown are representative brightfield microscopic images (bar=20 µm) from triplicate experiments.

Figure 3. Displacement of thrombin by Nb106 profoundly altering fibrin fibre structures but not clotting as such.

(**A-B**) Human plasma containing vehicle control medium or Nb106 (100 µg/mL) was triggered with TF (1-1000 pM), phospholipids and $CaCl_2$. (**A**) Effect of Nb106 on TF-induced mechanical (stirred) clotting time. (**B**) Abrogated TF-induced turbidity changes in coagulating plasma with Nb106 over time (**i**), plus quantification after 80 minutes (**ii**). Means ± SD (n=3-4 experiments, two-way ANOVA, non-parametric). (**C-E)** Atomic force microscopy (AFM) was employed for imaging of the fibrin protofibril assembly in preparations of human fibrinogen (0.5 mg/mL), $CaCl_2$ (2.5 mM) and thrombin (10 nM) in Tris-buffered saline, allowed to react for 10-60 seconds or 5 minutes. Control vehicle or Nb106 (100 mg/mL) was added to the

mixtures as indicated. Prepared samples on mica disks were examined with a Nanoscope IIIa MultiMode microscope operating in tapping mode. (**D**) Shown are representative images of fibrinogen, protofibril and polymerized fibrin molecules. Blue arrows indicate single molecule fibrin protofibrils. (**E**) Numbers of protofibrils per image of 2 x 2 mm. Mean ± SD (n=3-4, two-way ANOVA multiple comparison test). (**F**) End stage images after 5 minutes of fibrinogen cleavage. Note major reduction in size and length of fibrin fibres formed in the presence of Nb106.

Figure 4. Thrombogenic plasma profile in patients with congenital dysfibrinogenemia. Thrombin generation was compared in plasma samples from 21 patients with congenital dysfibrinogenemia (Table 1) and matching cohorts of healthy subjects (see Suppl. Figure 5), employing the same trigger conditions (1 pM TF, procoagulant phospholipids, $CaCl_2$), equipment and data processing. Plasmas were in part preincubated with Nb106 (150 µg/mL). (**A-F**) Comparative thrombin lag times (**A**, **D**), maximal thrombin (**D**, **E**) and thrombin capacities (**C**, **F**) in the absence or presence of Nb106. Medians and interquartile range (n=64 controls, Mann-Whitney U-test). (**G-I**) Plasmas from 21 patients and 25 healthy subjects were assessed for fibrinogen activity levels (Claus method), and for TF-triggered optical density changes or clot contraction with platelets from a healthy donor. Shown are scatter plots of thrombin capacity (**G**), clot contraction (platelet count: 200 × 10^9/L), (**H**), and turbidity changes (**I**), as a function of the fibrinogen level (patients in red, healthy subjects in black), for control samples. **(J-K)** Measured thrombin-antithrombin-III (TAT) complexes and active thrombin lifetimes of TF-triggered (60 minutes) individual control and patient samples (non-parametric Mann-Whitney U test).

Figure 5. Thrombin-enhancing effect of fibrin-derived synthetic peptides.

Functional analysis of synthetized peptide Pep1 consisting of residues 40-69 of fibrinogen-α and peptide Pep2 composed of residues 71-105 of fibrinogen-β (Suppl. Figure 7). (**A-F**) Thrombin generation assessed in normal pool plasma (NPP), fibrinogen-deficient plasma and antithrombin-III-deficient plasma (ATDP), measured with 500 μM peptide or vehicle medium after triggering with 1 pM TF. Shown are presentative traces (**A-C**) and quantified lagtime (**D**) maximal thrombin (**E**) and thrombin capacity level (**F**). (**G-H**) Peptide effects on kinetics of turbidity changes (**G**) and effect after 3-minutes (**H**) in normal plasma. (**I**) Microscopic images of fibrin structure after 20 minutes. (**J-K**) Combined peptide and Nb106 effects on thrombin capacity in NPP and ATDP, under conditions as in panels a-f. Mean ± SD (n=3). Statistically significant p values are shown in the figure (two-way ANOVA non-parametric).

Figure 6. Fibrin-bound thrombin affecting fibrin accumulation in mouse plasma and blood.

(**A-B**) Thrombin inhibiting and fibrin modifying effect of Nb106 in activated mouse plasma. (**A**) Mouse PRP was incubated with vehicle solution or Nb106 (100 µg/mL), and thrombin generation was induced with TF (1 pM), CRP (10 µg/mL) and $CaCl_2$ (16.6 mM). Shown are representative effects on thrombin generation over time (**i**), thrombin capacity (ETP) (**ii**), maximal thrombin level (**iii**) and thrombin lagtime (**iv**). Mean ± SD (n=4), non-parametric Mann-Whitney U test. (**B**) Mouse plasma containing Alexa Fluor 488-fibrinogen with(out) Nb106 (100 µg/mL) was triggered with 1 pM TF, phospholipids and $CaCl_2$ for confocal microscopic assessment of fibrin formation. Representative images recorded after 100 minutes. (**C-F**) Citrated mouse blood was supplemented with Alexa Fluor 488-fibrinogen (green) and Alexa Fluor 647-anti-GPIX mAb (purple), with Nb106 (100 µg/mL) present as

indicated. (**C**) Blood samples were continuously recalcified with 1 pM TF, while perfusing over collagen-I microspots at low, venous wall-shear rate of 200 s^{-1}. (**D**) Representative images of 6-min platelet deposition (AF647-α GPIX). (**E-F**) Quantification of fibrin surface area coverage and thrombus score on scale 1-6 over time.[20] Mean ± SD (n=4), non-parametric Mann-Whitney U test.

Figure 7. Schematized thrombin-fibrin interaction.

(**A-B**) Cartoons of human fibrinogen, adapted from Köhler et al. 2015[44]. (**A**) Duplicate proteins chains Aα, Bβ and γ in one fibrinogen molecule are represented in blue, red and green colours, respectively. Indicated are the D-E-D regions connected by coiled-coil regions. Represented is a molecule with single N-terminally thrombin-cleaved Aα and Bβ chains producing an FpA and FpB peptide. (**B**) Corresponding space-filled model based on the crystal structure of fibrinogen, also lacking FpA and FpB (PDB: 3GHG). (**C**) Drawing modified from the crystal structure of a fibrin central E region in complex with two thrombin molecules (PDB: 2A45). Central parts of the Aα, Bβ and γ chains are represented in blue, red and green colour, respectively. Gray area represent coiled-coil region. Attached thrombin molecules are shown in beige, with the active site in mustard, and exosite-I in orange. Adapted from Pechik et al.[13] (**D**) Global structure of a single chain antibody as model for Nb106. In colours, the three complementarity determining regions (CDR1-3) determining selective target (modified after Jacksonimmuno.com/camelid). (**E**) Proposed model of thrombin-fibrin interactions in the presence of Nb106, in normo- and dysfibrinogenemia or antithrombin-III deficiency, globally linked to thrombin activity.

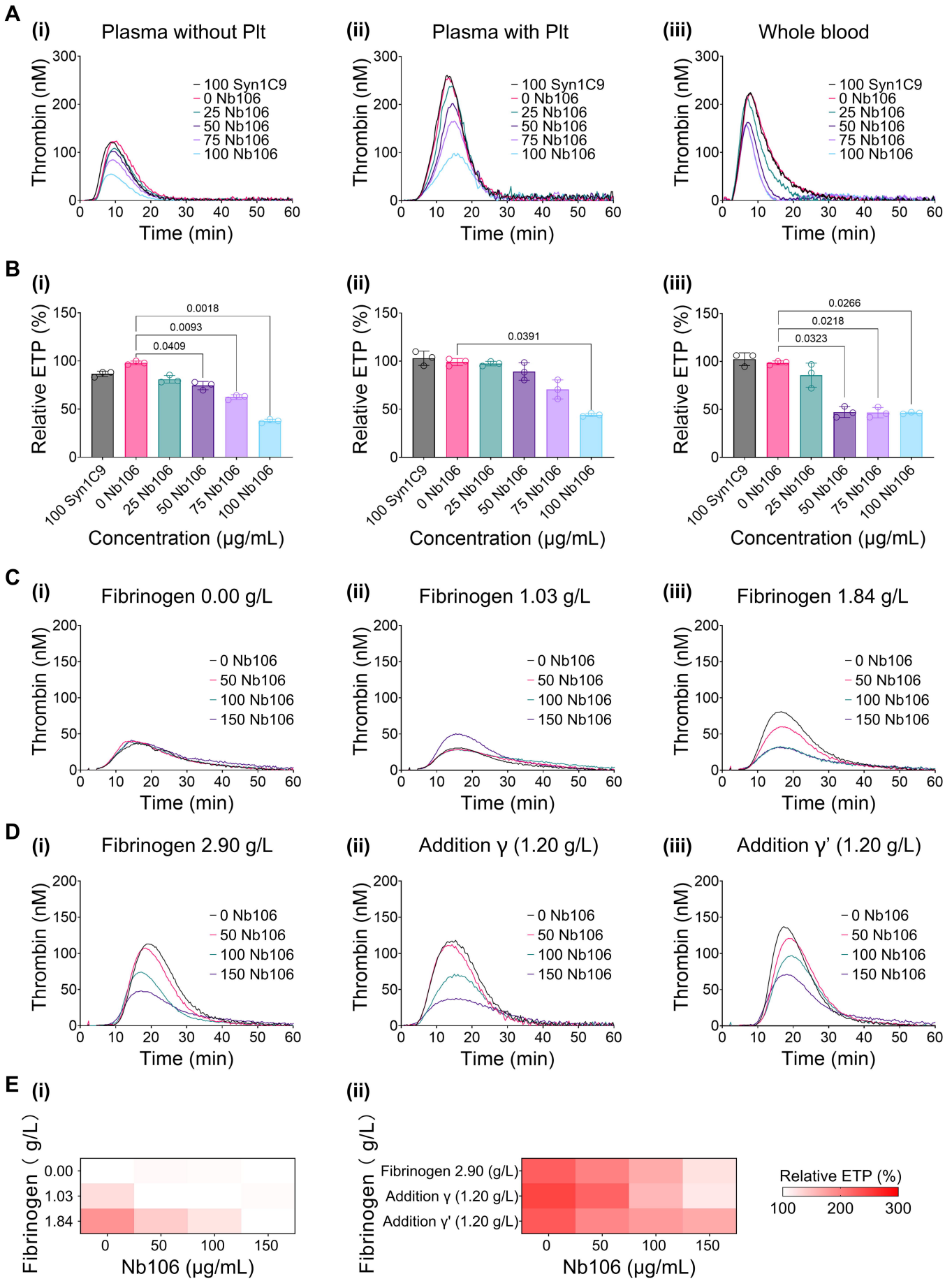
A
(i)
Plasma without Plt
(ii)
Plasma with Plt
(iii)
Whole blood
Thrombin (nM)
Time (min)
100 Syn1C9
0 Nb106
25 Nb106
50 Nb106
75 Nb106
100 Nb106
B
(i)
(ii)
(iii)
Relative ETP (%)
0.0018
0.0093
0.0409
0.0391
0.0266
0.0218
0.0323
Concentration (μg/mL)
C
(i)
Fibrinogen 0.00 g/L
(ii)
Fibrinogen 1.03 g/L
(iii)
Fibrinogen 1.84 g/L
0 Nb106
50 Nb106
100 Nb106
150 Nb106
D
(i)
Fibrinogen 2.90 g/L
(ii)
Addition γ (1.20 g/L)
(iii)
Addition γ' (1.20 g/L)
E
(i)
(ii)
Fibrinogen (g/L)
0.00
1.03
1.84
Nb106 (μg/mL)
Fibrinogen 2.90 (g/L)
Addition γ (1.20 g/L)
Addition γ' (1.20 g/L)
Relative ETP (%)

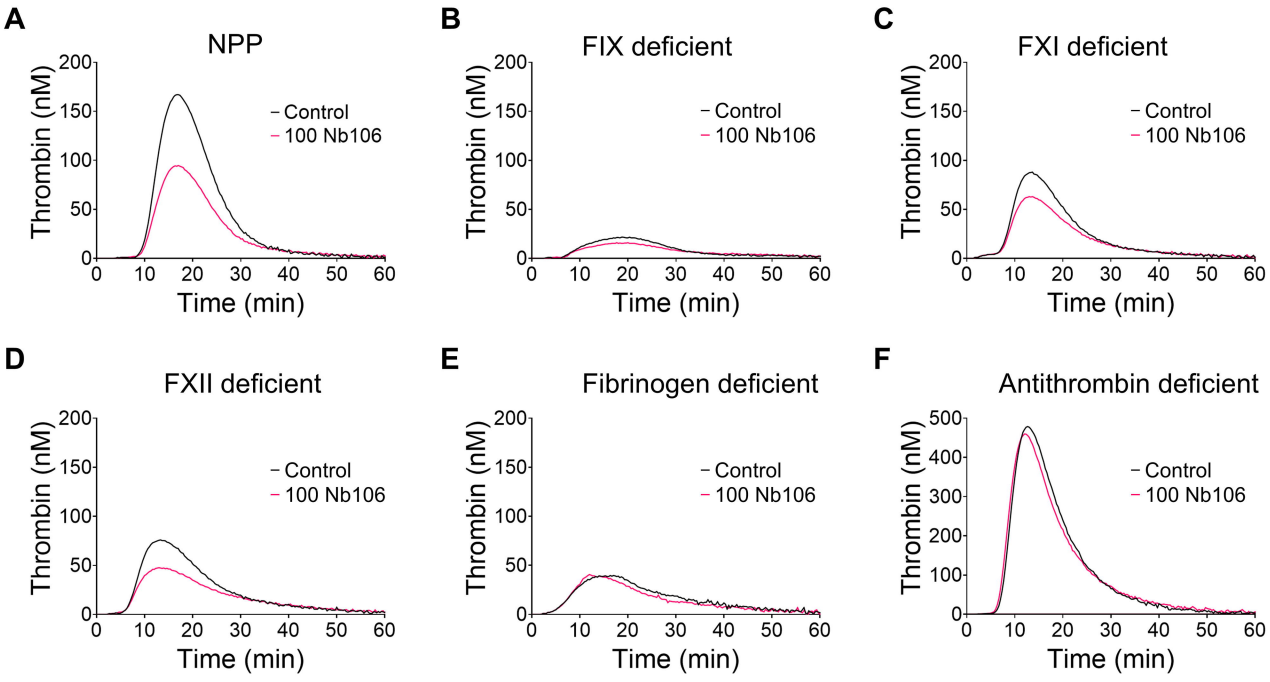

G

Factor deficiency	Effect of Nb106 (control 100%)					
	Relative lagtime (%)	*P*	Relative peak (%)	*P*	Relative ETP (%)	*P*
None (NPP)	104 ± 3	0.12	57 ± 8	0.003	62 ± 8	0.002
Fibrinogen	102 ± 3	0.37	102 ± 19	0.96	89± 11	0.20
Factor IX	104 ± 3	0.10	73 ± 4	0.004	85 ± 6	0.01
Factor XI	103 ± 2	0.12	72 ± 2	< 0.001	80 ± 1	< 0.001
Factor XII	102 ± 6	0.64	63 ± 4	0.001	75 ± 2	0.001
Antithrombin	95 ± 0.1	0.10	92 ± 4	0.12	97 ± 1	0.20

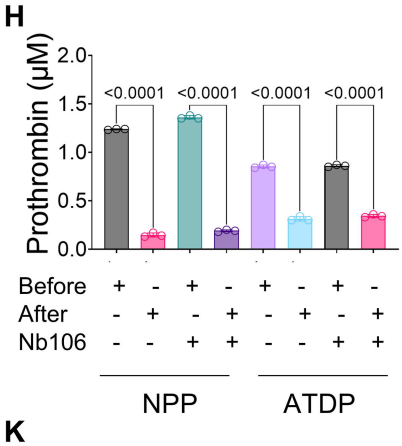

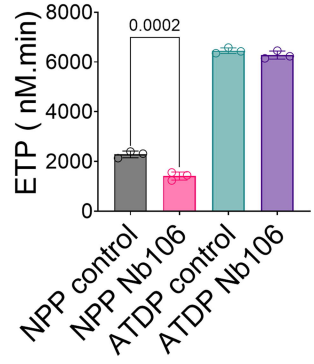

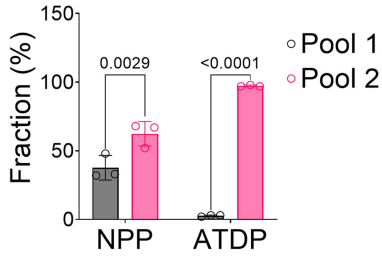

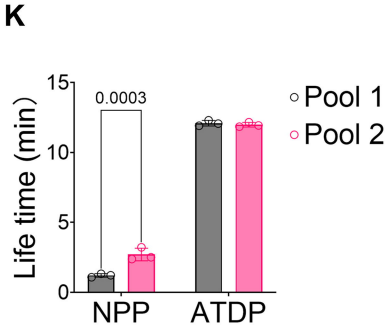

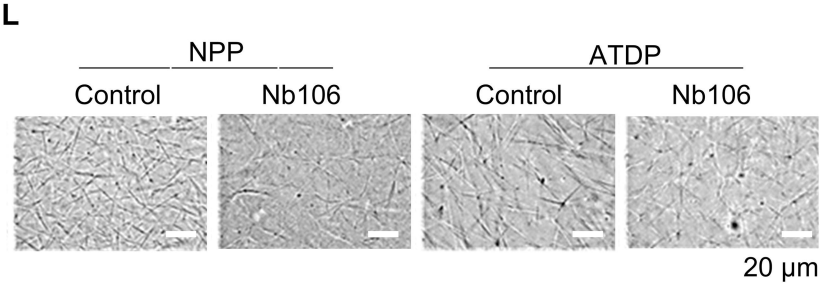

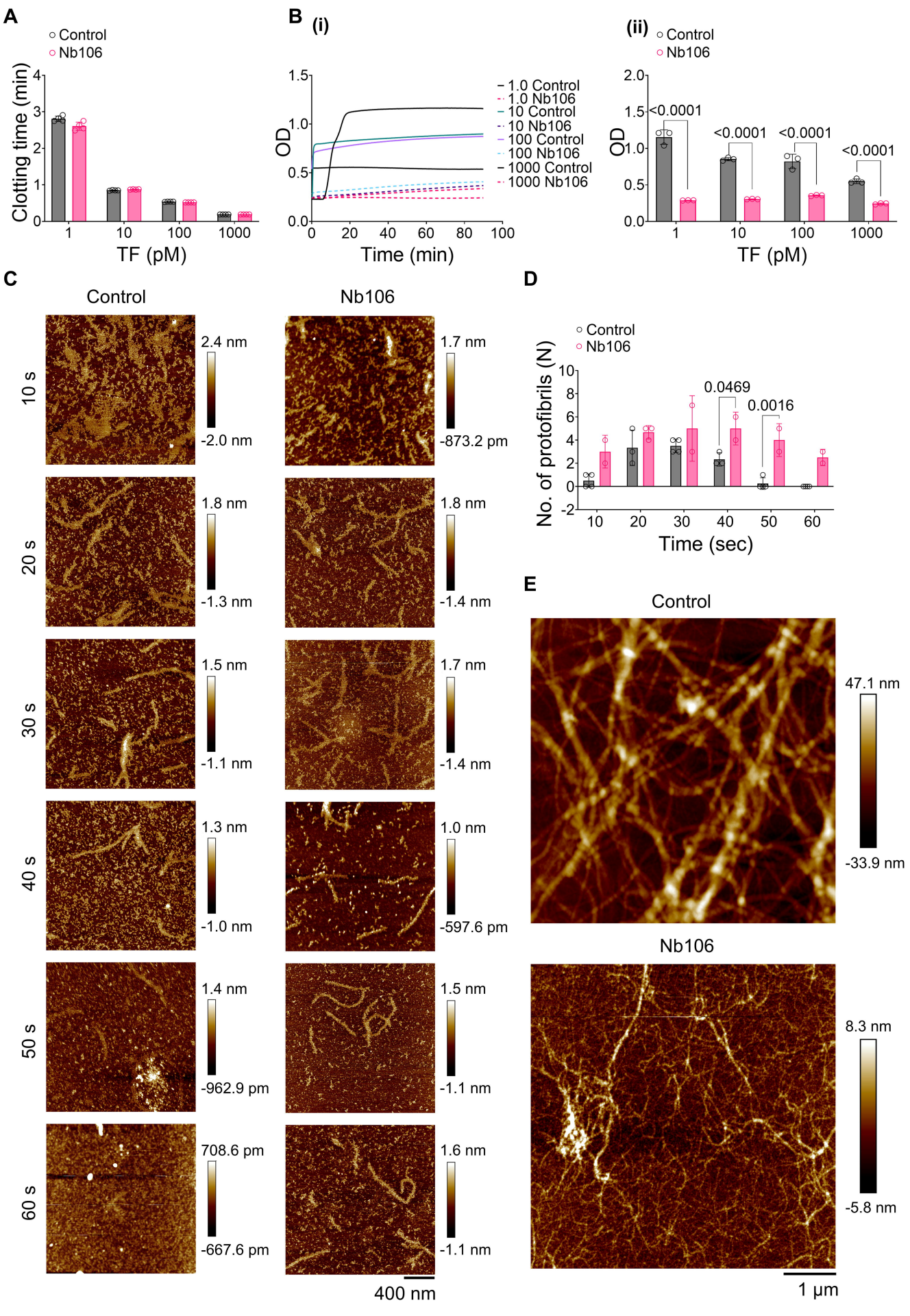
A
Control
Nb106
Clotting time (min)
TF (pM)
B
(i)
OD
Time (min)
1.0 Control
1.0 Nb106
10 Control
10 Nb106
100 Control
100 Nb106
1000 Control
1000 Nb106
(ii)
Control
Nb106
<0.0001
TF (pM)
C
Control
Nb106
10 s
20 s
30 s
40 s
50 s
60 s
2.4 nm
-2.0 nm
1.7 nm
-873.2 pm
1.8 nm
-1.3 nm
-1.4 nm
1.5 nm
-1.1 nm
1.3 nm
-1.0 nm
1.0 nm
-597.6 pm
1.4 nm
-962.9 pm
708.6 pm
-667.6 pm
1.6 nm
400 nm
D
Control
Nb106
No. of protofibrils (N)
0.0469
0.0016
Time (sec)
E
Control
47.1 nm
-33.9 nm
Nb106
8.3 nm
-5.8 nm
1 µm

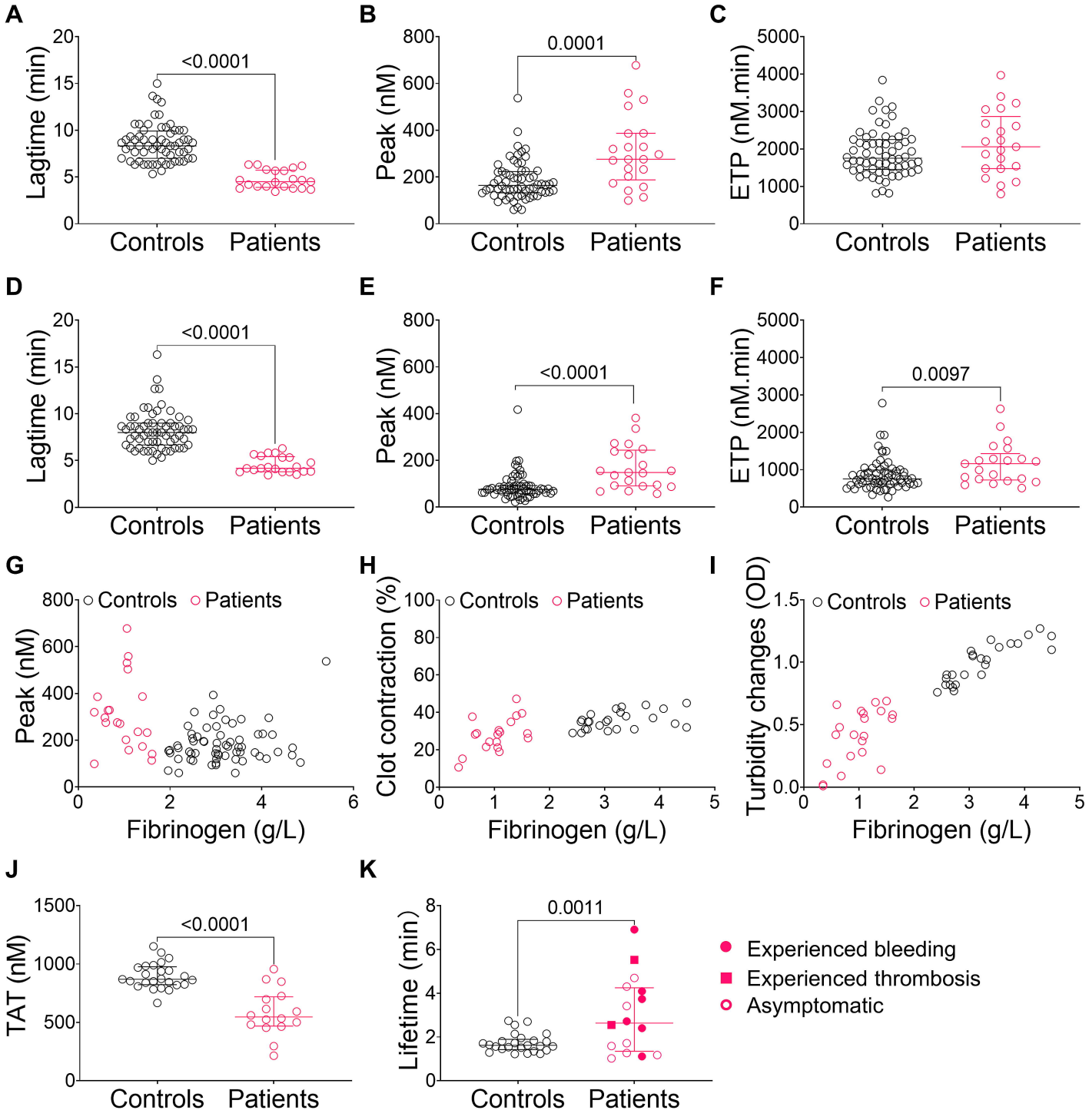
A
Lagtime (min)
<0.0001
Controls
Patients
B
Peak (nM)
0.0001
C
ETP (nM.min)
D
E
<0.0001
F
0.0097
G
Controls
Patients
Fibrinogen (g/L)
H
Clot contraction (%)
I
Turbidity changes (OD)
J
TAT (nM)
K
Lifetime (min)
0.0011
Experienced bleeding
Experienced thrombosis
Asymptomatic

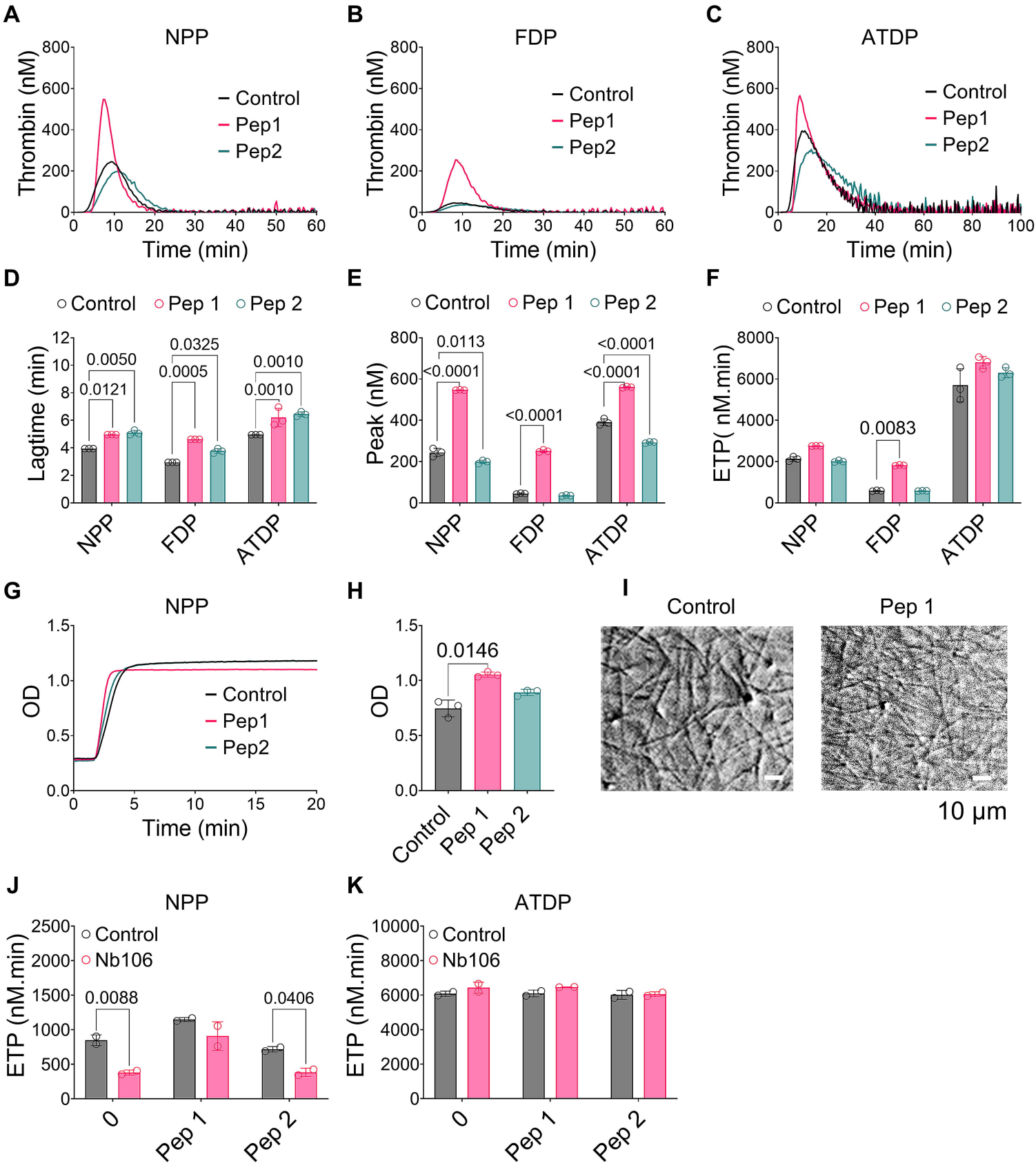
A
NPP
Thrombin (nM)
Time (min)
Control
Pep1
Pep2
B
FDP
C
ATDP
D
Lagtime (min)
0.0050
0.0121
0.0325
0.0005
0.0010
0.0010
E
Peak (nM)
0.0113
<0.0001
<0.0001
<0.0001
<0.0001
F
ETP(nM.min)
0.0083
NPP
FDP
ATDP
G
OD
H
0.0146
I
Control
Pep 1
10 μm
J
ETP (nM.min)
Nb106
0.0088
0.0406
K
0
Pep 1
Pep 2

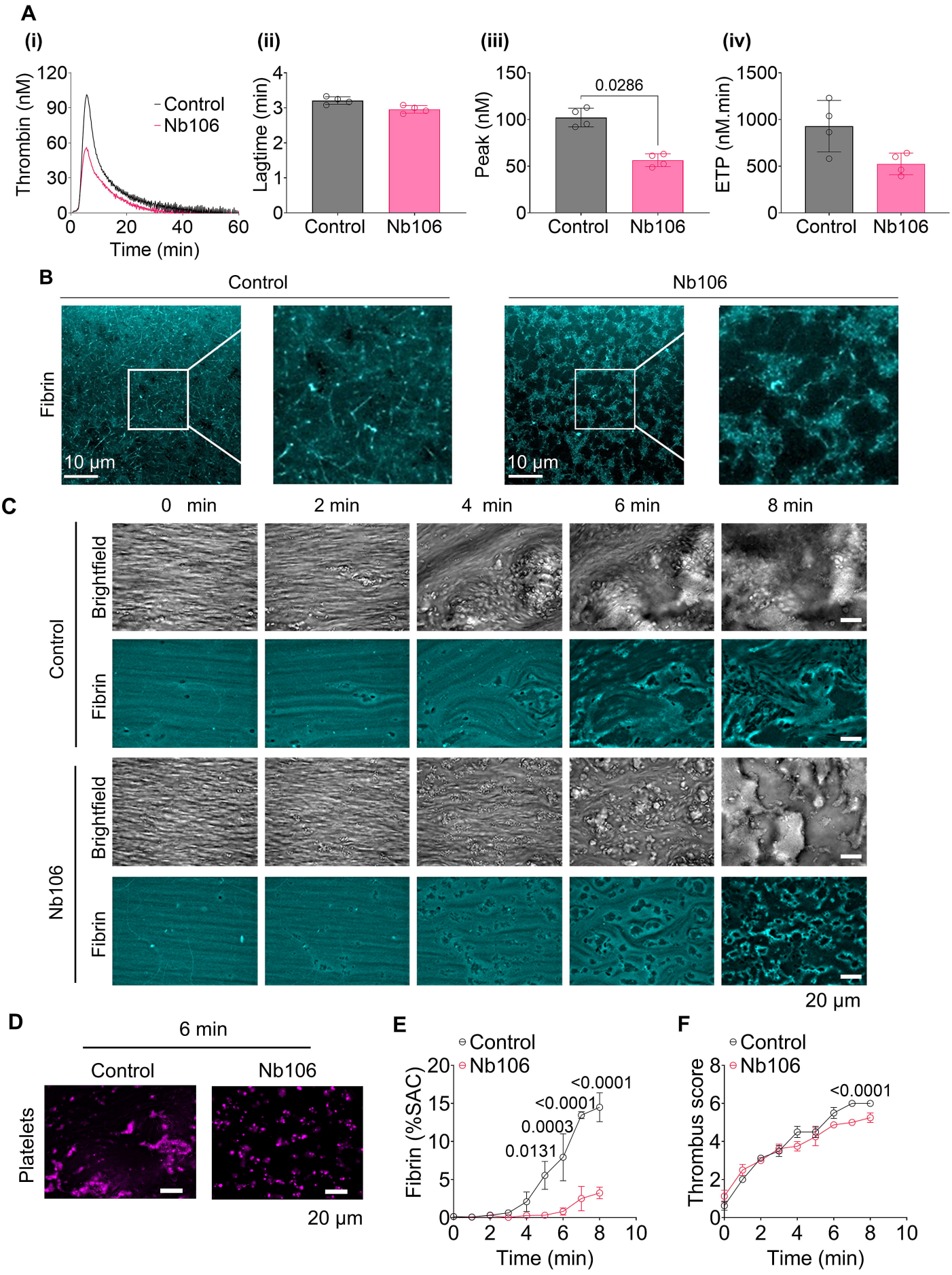
A
(i)
Thrombin (nM)
120
90
60
30
0
Control
Nb106
0
20
40
60
Time (min)
(ii)
Lagtime (min)
4
3
2
1
0
Control
Nb106
(iii)
Peak (nM)
150
100
50
0
0.0286
Control
Nb106
(iv)
ETP (nM.min)
1500
1000
500
0
Control
Nb106
B
Control
Nb106
Fibrin
10 µm
10 µm
C
0 min
2 min
4 min
6 min
8 min
Control
Brightfield
Fibrin
Nb106
Brightfield
Fibrin
20 µm
D
6 min
Control
Nb106
Platelets
20 µm
E
Control
Nb106
Fibrin (%SAC)
20
15
10
5
0
<0.0001
<0.0001
0.0003
0.0131
0
2
4
6
8
10
Time (min)
F
Control
Nb106
Thrombus score
8
6
4
2
0
<0.0001
0
2
4
6
8
10
Time (min)

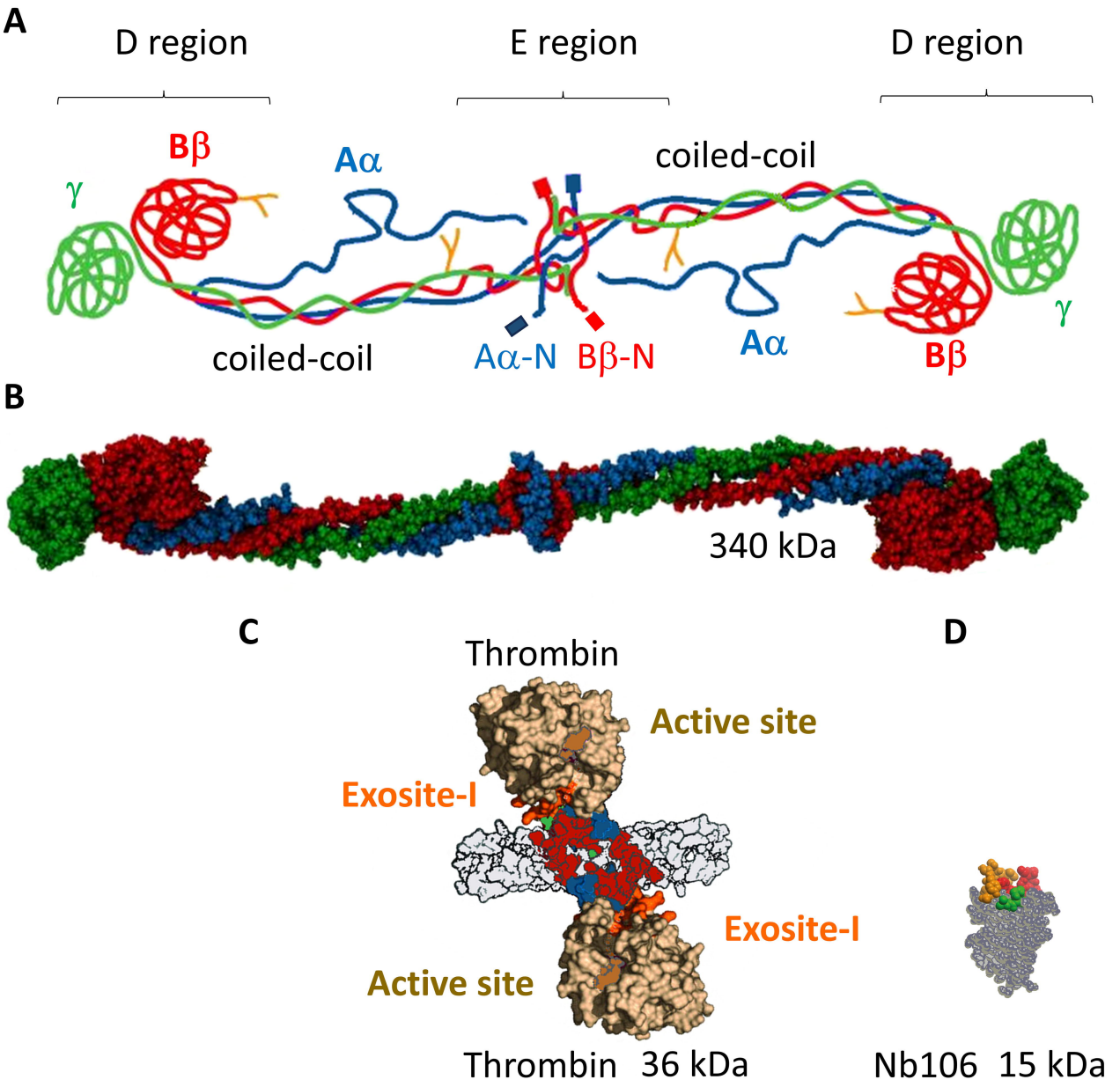
A
D region
E region
D region
Bβ
Aα
coiled-coil
γ
γ
γ
coiled-coil
Aα-N
Bβ-N
Aα
Bβ
B
340 kDa
C
Thrombin
Active site
Exosite-I
Exosite-I
Active site
Thrombin 36 kDa
D
Nb106 15 kDa
E
Nb106
Control
Dysfibrinogenemia
AT-III deficient
Lower thrombin capacity
Shortened thrombin lifetime
Higher thrombin capacity
Prolonged thrombin lifetime
Thrombin
Antithrombin-III
Fibrin fibre
Protofibril

SUPPLEMENT

Fibrin-bound thrombin determines clot structure and blood thrombogenicity in normofibrinogenemia and dysfibrinogenemia

Siyu Sun[1], Mark Roest[1*], Rolf T. Urbanus[2], Elena Campello[3], Sarah Beck[4], Cristiana Bulato[3], Simon D. Connell[5], Philip G. de Groot[1], Timea Feller[6], Dana Huskens[1], Joke Konings[1], Rita Marchi[7], Harmen Middelveld[1], Patricia Öftering[4], Bernhard Nieswandt[4], Alessandro Casini[7], Robert A. S. Ariëns[6], Paolo Simioni[3], Johan W. M. Heemskerk[1], Bas de Laat[1]

[1]Synapse Research Institute Maastricht, Kon. Emmaplein 7, 6217 KD, Maastricht, The Netherlands; [2]Van Kreveldkliniek, University Medical Centre Utrecht, The Netherlands; [3]Department of Medicine, University of Padua, Padova, Italy; [4]Rudolf Virchow Center for Integrative and Translational Bioimaging & Institute of Experimental Biomedicine, Julius-Maximilians-Universität Würzburg, Germany; [5]Molecular and Nanoscale Physics Group, School of Physics, University of Leeds, Leeds, UK; [6]Discovery and Translational Science Department, Leeds Institute of Cardiovascular and Metabolic Medicine, University of Leeds, Leeds, UK; [7]Division of Angiology and Hemostasis, Department of Medicine, University Hospitals of Geneva, University of Geneva, Switzerland.

Supplemental Methods

Chemicals

Recombinant tissue factor (TF, Innovin) was purchased from Siemens Healthineers (Marburg, Germany); fluorogenic substrate Z-Gly-Gly-Arg-aminomethyl coumarin (ZGGR-AMC) and peptide GPRP from Bachem (Bubendorf, Switzerland). Thrombin calibrator (α2-macroglobulin-thrombin complex), human thrombin, protease III and activated protein C were prepared in-house by Synapse Research Institute (Maastricht, The Netherlands).[1,2] Synthetic phospholipid mixture consisting of 20 mol% phosphatidylserine, 20 mol% phosphatidylethanolamine and 60 mol% phosphatidylcholine was from Avanti Polar Lipids (Alabaster, AL, USA). Alexa Fluor-647 anti-glycoprotein IX antibody (56F8) and Alexa Fluor-488 fibrinogen were purchased from Invitrogen Life Technologies (Budapest, Hungary). Purified ancrod was from Knoll (Ludwigshafen, Germany); chromogenic substrate S2238 from Chromogenix (Brussels, Belgium). Staphylocoagulase was purified in house, as described by Hendrix et al.[3] Echis carinatus venom was obtained from Sigma-Aldrich (Darmstadt, Germany). Obtained from Invitrogen Life Technologies (Burlington, Canada) were thrombin exosite 1 and 2-directed DNA aptamers, Apt1 (GGTTGGTGTGGTTGG, HD1) and Apt2 (AGTCCGTGGTGGTAGGGCAGGTTGGGGTGACT, HD22), and the exosite 1-2-directed aptamer Apt3 (combined HD1 and HD22: GGTTGGTGTGGTTGG-AAAAAAAAAAAAAAA-AGTCCGTGGTGGTAGGGCAGGTTGGGGTGACT). The FGA/FGB-derived peptides, Pep1 (SACKDSDWPFCSDEDWNYKC) and Pep2 (YRARPAKAAATQKKVERKAPDAGGCLHADPDLGVL), were chemically synthetized by Synpeptide (Nanjing, Jiangsu, China). Cross-linked collagen-related peptide (CRP-XL), as a platelet GPVI) agonist, came from CambCol (Cambridge, United Kingdom), and direct oral anticoagulant dabigatran was from Alsachim (Illkirch-Graffenstaden, France).

Normal pool plasma (NPP) was prepared in house.[4] Antithrombin-deficient plasma came from Hematologic Technologies (Essex Junction, VT, USA). Plasmas deficient in fibrinogen, factor IX, XI or XII were bought from Affinity Biologicals (Ancaster, Canada). A purified preparation of fibrinogen γ' was used, as described before.[5]

Antibodies

The single chain antibody Nb106 was generated in-house from a llama injected with fibrin degradation products, enriched in fibrin D-D and D-E-D dimers, according to described

procedures.[6,7] It was selected for binding to human fibrin monomers but not un-cleaved fibrinogen. The non-responsive single chain antibody Nb-Syn1C6 was raised similarly. Single chain antibody against human antithrombin was obtained from Biointron Biological (Shanghai, China).

Human blood donors and blood sample preparations

Studies with blood from healthy donors were approved by the Medical Ethical Committee of Maastricht University Medical Centre (NL31480.068.10). Patient studies were approved by the Research and Ethics Committees of Padua University Hospital Italy (protocol code 4303/AO17, July 28, 2017) and of the University Hospitals of Geneva (Switzerland). Studies were conducted in accordance with the Declaration of Helsinki. Blood donors had not taken anticoagulant or antiplatelet medication for at least two weeks, and gave written informed consent. Congenital dysfibrinogenemia was classified from a reduced fibrinogen activity level in comparison to the antigen level. Genotyping followed the International Society of Thrombosis and Haemostasis classification.[8] Screenings for *FGA*, *FGB* and *FGG* mutations were based on suspected dysfibrinogenemia, and were performed by PCR amplification of fibrinogen coding sequences, followed by Sanger sequencing.[9] Mutations were annotated as described in the Human Genome Variation Society guidelines. Gene nucleotide numbering was according to NIH GenBank sequences.

All human blood samples (9 volumes) were taken from the antecubital vein and were drawn into aseptic vacutainer tubes (Greiner Bio-One, Alphen a/d Rijn, The Netherlands), containing 3.2% sodium citrate (1 volume). The samples kept at room temperature were used within 2-3 h for experiments or plasma preparation. Routinely, blood cell parameters were measured with a cell counter analyser (SthemA 601, Stago, France). Platelet counts in the healthy subjects were within the normal range (150-400 × 10^9/L).

Platelet-rich plasma (PRP) and washed platelets were prepared, as outlined before.[2,10] In brief, PRP was obtained by centrifuging blood for 15 minutes at 250 g. For collecting washed platelets, PRP was supplemented with 10 vol% ACD medium (80 mM trisodium citrate, 52 mM citric acid and 180 mM glucose), after which the cells were spin down in 2 mL Eppendorf tubes at 1700 g for 2 minutes. After plasma removal, pellets were resuspended into 1 mL of Hepes buffer pH 6.6 (136 mM NaCl, 5 mM Hepes, 2.7 mM KCl, 2 mM $MgCl_2$, apyrase at 0.2 unit ADPase/mL, 0.1% glucose and 0.1% bovine serum albumin). After another addition of ACD, the tubes were recentrifuged. Washed platelets were resuspended per tube into 1 mL Hepes

buffer pH 7.45 (10 mM Hepes, 136 mM NaCl, 2.7 mM KCl, 2 mM $MgCl_2$, 0.1% glucose, and 0.1% bovine serum albumin).

Citrated blood samples, collected by venipuncture, from control subjects and patients were subjected to double centrifugation at 2000 g for 15 minutes at room temperature. Within 2 hours after blood sampling, plasmas were aliquoted and stored as at −80 °C until use. For cohort testing, plasmas were obtained from 64 healthy individuals, as described.[11] Included were samples from 28 males and 36 females, with mean ages of 34 and 32, respectively.

Mouse blood

Adult wildtype C57BL/6 mice (males and females) were maintained under specific pathogen-free conditions, as described before.[12] Experiments were performed in accordance with German law, and permission was obtained from the Animal Experimental Ethics Committee from the District of Lower Franconia (Germany). Mouse blood was obtained by orbital puncture, and collected into citrate anticoagulant.[12,13] Whole blood samples were used for microfluidic testing or for plasma preparation, as detailed elsewhere.[14]

Thrombin generation assessment

Using a 96-well-plate based method of calibrated thrombin generation (37 °C), the formation and ensuing inactivation of thrombin was monitored in centrifuged plasma or PRP samples, employing a low-affinity fluorogenic substrate for thrombin, which does not interfere with the coagulation process.[10,15] In brief, wells contained 80 µL plasma or PRP plus 20 µL of trigger solution: 1 pM TF and 4 µM procoagulant phospholipids, dissolved into BSA5 buffer (20 mM Hepes, 140 mM NaCl, 5 mg/mL bovine serum albumin, pH 7.35). In experiments with PRP, phospholipids were left out, as platelets provided the procoagulant membranes. Coagulation was started by dispensing 20 µL of substrate solution, consisting of 11 mM $CaCl_2$, 5.5 mM $MgCl_2$ and 417 µM Z-GGR-AMC, dissolved into BSA60 buffer (20 mM Hepes, 140 mM NaCl, 60 mg/mL BSA, pH 7.35). For each plasma type, additional wells were used, in which the trigger solution was replaced by a thrombin calibrator. Calibration curves corrected for effects of plasma colour, and allowed conversion of fluorescence levels (nonlinear if required) into nanomolar thrombin concentrations.[16] First-derivative thrombin generation curves provided levels of thrombin lag time (min), maximal thrombin concentration (nM), and thrombin capacity (area-under-the-curve = ETP in nM x min).[4] Samples in wells were pre-incubated with

modulating agents for 10 minutes at 37°C.

For whole-blood thrombin generation, citrated blood samples were thoroughly mixed with substrate solution (Z-GGR-AMC dissolved into BSA60 buffer) and trigger solution (1 pM TF, 6 mM $CaCl_2$ and 3 mM $MgCl_2$ dissolved into BSA5 buffer).[4] The volume ratio of blood, trigger solution and substrate solution was 3:2:1. A modified Excel-based template was used to obtain calibrated, first derivative thrombin generation curves.

Plasma thrombin pool assessment

To estimate thrombin pools, wells of round bottom 96-well plates were used without additional coating. Plasma samples were preincubated with Nb106 or vehicle buffer for 10 min at 37 °C, before measuring thrombin generation, which was commonly triggered with $CaCl_2$/$MgCl_2$, phospholipids and tissue factor.

For the assessment of prothrombin consumption, prothrombin levels were measured both before and after 60 min of tissue factor addition. Measurements were carried out in diluted subsamples using a molar excess of staphylocoagulase, *i.e.* a venom that exposes the catalytic site of prothrombin.[17] To reach a molar excess of staphylocoagulase, the overall plasma dilution was 1:400, as described.[18] Staphylocoagulase-activated prothrombin in the diluted samples was quantified using the chromogenic substrate S2238. Included were separate control samples with Nb106 added to the plasma prior to dilution. Note that the Nb106 concentration in the assayed diluted plasma samples was around 250 ng/mL.

Average thrombin lifetimes were calculated as the ratio of the total amount of thrombin generated during 60 minutes (ETP, nM·x min) to the amount of prothrombin consumed over the same period. This calculated lifetime hence represents the average duration during which thrombin remains proteolytically active over 60 minutes. This endpoint-based approach correlated well with reported kinetic lifetime values of antithrombin-deficient plasma, and allowed direct comparison with thrombin–antithrombin complex measurements. Average lifetimes of two reactive thrombin pools were calculated, assuming that pool 2 consisted of selectively displaced thrombin from fibrin by a saturating concentration of Nb106:

(1) $$\text{Fr. Pool 1} = \frac{\text{TC}_{\text{Nb106}}}{\text{TC}_{\text{Con}}}$$

(2) $$\text{Fr. Pool 2} = 1 - \frac{\text{TC}_{\text{Nb106}}}{\text{TC}_{\text{Con}}}$$

(3) $$\text{PC (Prothrombin consumption)} = \text{Prothrombin}_{\text{plasma}} - \text{Prothrombin}_{\text{serum}}$$

(4) $$\text{Lifetime in pool 1} = \frac{\text{TC}_{\text{Nb106}}}{\text{PC}_{\text{Nb106}}}$$

(5) $$\text{Lifetime in pool 2} = \frac{\frac{\text{TC}_{\text{Con}}}{\text{PC}_{\text{Con}}} - \text{lifetime in pool 1} \times \text{Fr. Pool 1}}{\text{Fr. Pool 2}}$$

Herein, "Fr. Pool 1" represents the thrombin capacity (TC) fraction of thrombin in pool 1, and "Fr. Pool 2" the fraction in pool 2.

Prothrombin clotting time

Normal pool plasma (NPP) was preincubated with Nb106 (100 µg/mL) or vehicle (control) for 10 min at 37°C. Clotting was triggered with 1-1000 pM TF, 4 µM procoagulant phospholipids, 11 mM $CaCl_2$ and 5.5 mM $MgCl_2$. Plasma clotting times were measured using a STart apparatus (Stago, Paris, France).

Clot turbidity assay

Fibrin-dependent turbidity changes in clotting plasma were monitored for 50 minutes in triplicate in 96-well plates, using spectrophotometric recording (SpectraMax, Molecular Devices, Salzburg, Austria) of the optical density at 405 nm.[19] For coagulation induction, samples of plasma from healthy subjects or patients were mixed with 1 pM TF, 4 µM procoagulant phospholipids, 11 mM $CaCl_2$ and 5.5 mM $MgCl_2$.

Plasma fibrinogen assessments

Active fibrinogen concentrations in plasmas were measured by the Clauss method by triggering with purified human thrombin.[9] Plasma levels of fibrinogen were measured by conventional immunoassay on a standard coagulometer. Levels were expressed as antigen levels (g/L) or as percentages of mean of controls of 3.0 g/L. For functional fibrinogen measurements (Claus method), reference values were 1.5-4.5 g/L, for fibrinogen antigen 2.4-3.6 g/L (80-120%).[20]

Clot contraction

To measure clot formation and contraction, samples of reconstituted PRP (platelet count: 200 × 10^9/L) preincubated with Nb106 (100 µg/mL) or vehicle (control) were triggered with 1 pM TF and 10 mM $CaCl_2$.[21] Clotting was monitored in 1 mL TH-CV-1000 glass tubes (SD Innovation, Frouard, France) at 37 °C, which were imaged for up to 150 minutes. The images were analysed for pixel surface-area-coverage (SAC%) of visible clots, using a home-made Fiji script.

Light transmission and confocal microscopy

Normal pool plasma (NPP) and antithrombin-III depleted plasmas were preincubated with Nb106 (100 µg/mL) or vehicle (control) for 10 minutes at 37 °C. Fibrin formation was then triggered with 1 pM TF, 4 µM phospholipids, 11 mM $CaCl_2$, and 5.5 mM $MgCl_2$. After thorough mixing, the mixture was immediately transferred to a glass slide and the fibrin formation was observed with an inverted light transmission microscope with 63x objective (Leica DFC 3000 G, Wetzlar, Germany). Confocal microscopy of fibrin structures was performed, as described elsewhere.[12]

Atomic force microscopy of single molecule and polymerized protofibrils

Atomic force microscopy (AFM) was employed for the imaging of fibrin protofibril and fibril assembly, as detailed previously. In brief, purified fibrinogen (0.5 mg/mL), $CaCl_2$ (2.5 mM) and Nb106 (100 µg/mL) or vehicle control solution were mixed to obtain 20 µL sample volumes. After addition of thrombin (10 nM), reactions were stopped in concatenated samples, with interval of 10 seconds, by addition of 1480 µL of Tris-buffered saline. Subsamples of 50 µL were deposited onto mica discs (pre-treated with 2 mM $NiCl_2$ for 10 minutes). For end-stage measurements, fibrinogen (final concentration 0.5 mg/mL), $CaCl_2$ (2.5 mM) and TBS buffer were pre-mixed in a final volume of 20 µL, and transferred to freshly cleaved mica discs (pre-treated with 2 mM $NiCl_2$ for 10 minutes). After adding thrombin (10 nM), the solution was spread on the disc surface. Samples were allowed to clot for 5 minutes. Before AFM imaging, discs were rinsed with dH_2O and dried under nitrogen gas. The fibrin samples were imaged with a Nanoscope IIIa MultiMode AFM (Veeco Instruments, Santa Barbara, CA, USA), operated in tapping mode. Image processing and analysis was using Nanoscope software (Veeco Instruments).

Peptides and aptamers for testing interference with thrombin

Based on established binding of thrombin to N-terminal regions of fibrin Aα and Bβ chains,[22]

two novel peptides were designed corresponding to these sites, which were synthesized (>95% purity) by Synpeptide (Nanjing, Jiangsu, China). The constructed 30 amino-acid peptide-1 (Pep1) consisted of residues 40-69 of the full-length product of wildtype human *FGA* (3.65 kDa). The 35 amino-acid peptide-2 (Pep2) consisted of residues 71-105 of the product of wildtype human *FGB* (3.78 kDa). Aptamer 1 of 4.88 kDa (blocking thrombin exosite I), aptamer 2 of 10.4 kDa (blocking thrombin exosite II), and aptamer 3 of 20.2 kDa (blocking thrombin exosites I and II) were used, as before.[4]

Thrombin-antithrombin complex assessment

Thrombin-antithrombin (TAT) complex levels were measured using a high-throughput enzyme-linked immunosorbent assay (ELISA), essentially as described.[23] In short, 384-well microliter plates were coated overnight at 4 °C with 2 µg/mL novel single domain antibody against antithrombin Nb1024, fused with an Fc-tail (Synapse Research Institute, Maastricht, The Netherlands), in carbonate-bicarbonate coating buffer pH 9.6. The wells were then blocked with phosphate-buffered saline pH 7.4 containing 20 mg/mL BSA and 0.05% Tween-20 for 2 hours at room temperature. After washing, activated plasma samples (diluted 1:20 in phosphate-buffered saline containing 10 mg/mL BSA) were added and incubated for 2 hours. Hereafter, the wells were incubated overnight with peroxidase-conjugated anti-prothrombin polyclonal antibody (1:10000 dilution; Affinity Biologicals, Ontario, Canada) for assessment of TAT levels. Plates were then washed with phosphate-buffered saline containing 0.05% Tween-20 before addition of SuperSignal West Femto Maximum Sensitivity substrate (ThermoFisher). Luminescence was measured with a Synergy H1 multimode microplate reader (Biotek, Bad Friedrichshall, Germany). Signals were converted into molar levels of TAT using a calibration curve of prothrombin.

Reactive thrombin lifetime for a given activated plasma sample was calculated from the 60-minutes thrombin capacity level (nM x min) from calibrated thrombin generation curves and the 60-minutes TAT concentration (nM) at the same activation conditions.

Ex vivo thrombus formation during whole blood flow

Whole-blood thrombus formation to observe platelet-dependent fibrin clotting under flow conditions (wall shear rate of 200 or 1000 s^{-1}) was assessed, basically as described for mouse blood[12] or for human blood.[13] In all cases, a transparent parallel-plate microfluidic chamber was used containing a coverslip with microspots of collagen-I.[24] Citrate-anticoagulated blood

samples were flowed over the surface upon continuous recalcification using a y-shaped dual inlet system, connected to two pulse-free perfusion pumps.[25] Optimal coagulation was obtained by co-infusion of the blood samples 10:1 (vol/vol) with recalcification medium (1 pM TF, 3.75 mM $MgCl_2$ and 7.5 mM $CaCl_2$). Blood samples were pre-incubated with control vehicle or with Nb106. as indicated.

For mouse flow studies, blood samples were prelabelled with Alexa Fluor-647 anti-glycoprotein IX antibody (clone 56F8) plus Alexa Fluor-488 fibrinogen.[12] Recording was with a Leica DMI 6000 B fluorescence microscope, equipped an 63x oil-immersion objective. The images were processed with an Instant Computational Clearing method to remove out-of-focus background blur.[12] For human flow studies, blood samples were prelabelled with Alexa Fluor-647 fibrinogen.[25] Recording was with an inverted EVOS fluorescence microscope, containing an Olympus 60x oil-immersion objective with high z-axis resolution and an 8-bit monochrome camera. Images were semi-automatically processed by scripts in the AForge. NET image processing library.[26]

Preparation of PPACK–thrombin complex

PPACK–thrombin was prepared by mixing human α-thrombin with PPACK at a 1:1 molar ratio. The reaction mixture was incubated for 30 minutes at room temperature. Unreacted PPACK was removed by chromatography using a desalting column (HiTrap desalting on Sephadex G-25 resin, 5 mL), pre-equilibrated with Hepes buffer pH 7.45. The concentration of PPACK–thrombin was determined spectrophotometrically at 280 nm using an extinction coefficient of 1.83.

To confirm complete inhibition of thrombin activity, 1 µL of the purified PPACK–thrombin mixture was diluted into 499 µL BSA 5 buffer. A total of 125 µL of the diluted sample was transferred to a 96-well microplate, followed by the addition of 25 µL of S-2238 substrate solution (600 nM). Absorbance changes at 405 nm were recorded to monitor thrombin activity. The absence of residual free PPACK was determined by incubating 2 µL of the purified PPACK–thrombin preparation with 20 µL of active thrombin (10 nM) and 478 µL of BSA 5 buffer. Then, 125 µL of the mixture was added to a 96-well microplate, followed by the addition of 25 µL S-2238 substrate solution. Again, changes in absorbance at 405 nm were measured.

Data analysis

Statistical analyses were performed with GraphPad Prism 9 (San Diego, CA, USA). Data are

presented as mean ± SD, unless indicated otherwise. For normally distributed datasets, unpaired two tailed Student's t tests were used. Multiple groups were compared using a one-way ANOVA (Kruskal-Wallis test) followed by post-hoc testing for multiple comparisons. Inter-group interactions were analysed using two-way ANOVA with Sidak's correction. In the absence of normality, a Mann–Whitney U test was used for comparisons between two groups. Values of $p < 0.05$ were considered as statistically significant.

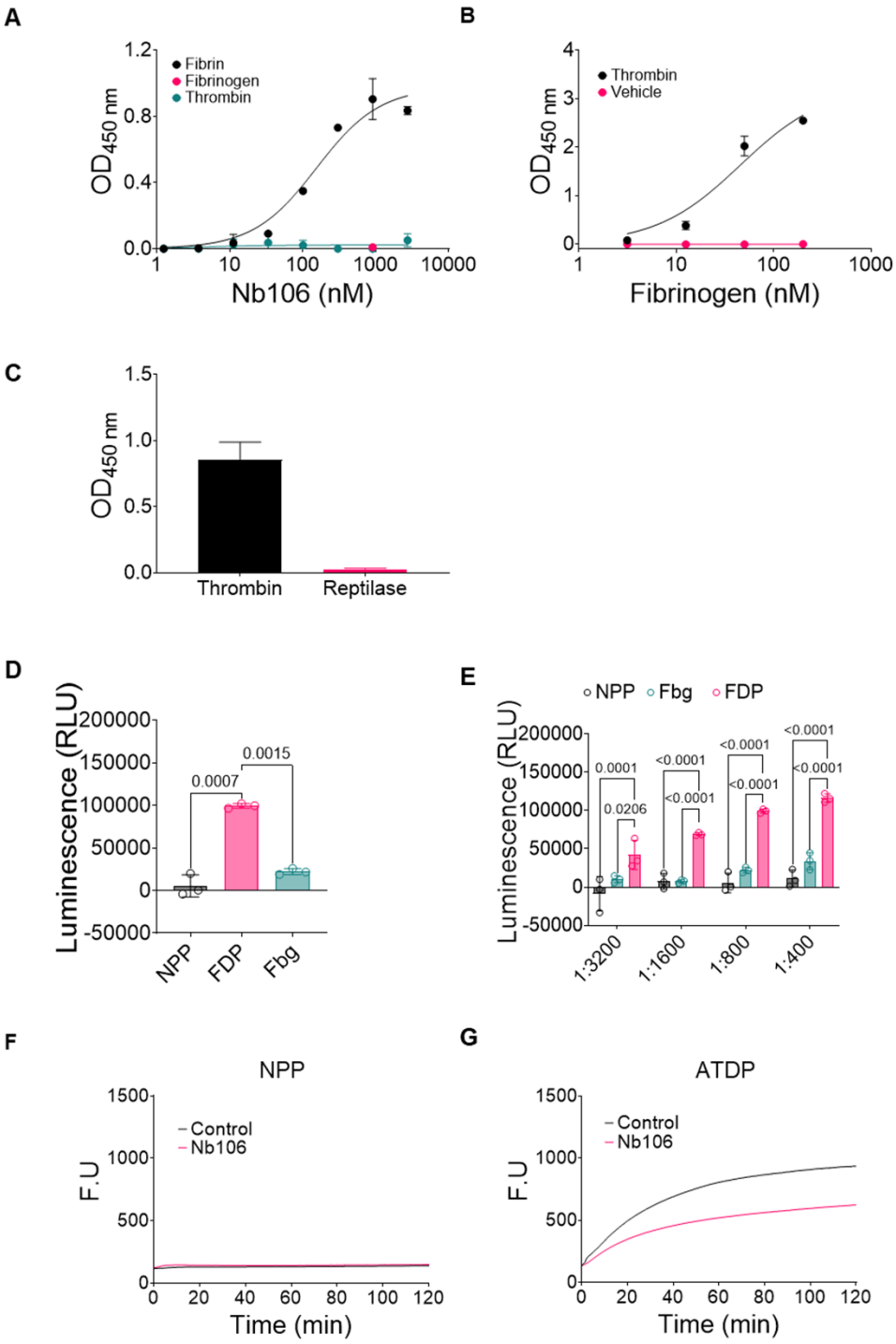

Suppl. Figure 1. Binding characterization studies of the selected single-chain antibody Nb106. (**A**) Nb106 binding to immobilized fibrin, but not fibrinogen or thrombin. In 96-wells, fibrinogen (10 µg/mL) plus thrombin (50 µg/mL) were coated overnight to form fibrin, while other wells contained only fibrinogen of thrombin. Plates were thoroughly washed with phosphate-buffered saline (PBS) containing 0.1% Tween-20 (PBS-T), and incubated with crude Myc-tagged single-chain antibodies for 1 hour. Antibody (Ab) binding was detected with 1 µg/mL mouse anti-c-Myc mAb (clone 9E10, purified in-house), followed by horse radish peroxidase (HRP)-labeled rabbit anti-mouse-Ab (1:1000, Daka, Santa Clara, CA, USA). Plates were stained with 3,3'5,5'-tetramethylbenzidine (Pierce, Appleton, WI, USA), with an acid stop

using 0.1 M H_2SO_4. Coloring was read at 450 nm. Results are shown for single chain c-Myc Nb106, which was selected from 10 clones with selective binding to immobilized fibrin only (total of 138 clones). (**B**) Binding of Nb106 to fibrin monomers. Wells were coated with anti-c-Myc Ab (1 µg/mL) in carbonate buffer, blocked with 2% skimmed milk in PBS for 1 hour, and incubated with purified Nb106 (5 µg/mL) in blocking buffer. After washing, the wells were incubated with fibrin monomers (thrombin) or fibrinogen (vehicle) at indicated concentrations. Fibrin monomers were made by incubating fibrinogen (200 nM) with thrombin (20 nM) and GPRP (200 µM) in blocking buffer. Serial dilutions of fibrin monomers were made in blocking buffer. After thorough washing and blocking with 2% albumin, fibrin monomers were detected in the presence of 200 µM GPRP. Detection was with rabbit anti-fibrinogen mAb (1:2000, Dako), followed by HRP-labeled swine-anti rabbit Ab. Plates were developed as described for panel A. Calculation showed an apparent KD for Nb106 46 nM, which is an underestimate due to the various washing steps. (**C**) Abolished Nb106 binding to fibrin formed by cleavage of only fibrinopeptide FpA. Wells were coated with anti-fibrinogen mAb (1:5000), blocked with 2% albumin, thoroughly washed, incubated with fibrinogen (300 µg/mL) for 1 hour, and washed again. Some wells were then incubated with thrombin (20 nM) or reptilase (25 µg/mL, cleaving FpA at Arg16-Gly17 but not FpB). After a wash, treatment with PPACK (50 µM) and another wash step, the wells were incubated with Nb106 (10 µg/mL), and stained as described for panel A. (**D-E**) Selective binding of Nb106 to plasmin-treated fibrin, but not fibrinogen. Coated Nb106 (10 µg/mL) was incubated with normal pool plasma (NPP), with plasma containing fibrin degradation products (FDP), or with purified fibrinogen (Fbg). (**D**) Paratope binding was detected via ELISA using an HRP-conjugated polyclonal anti-fibrinogen Ab. Shown are relative luminescence units(RLU), means of triplicates. (**E**) Paratope binding after incubation with indicated dilutions of NPP, FDP or Fbg. (**F-G**) Thrombin displacement from coated fibrin by Nb106. In-situ coated fibrin (50 µg/mL fibrinogen plus 20 nM thrombin, 30 minutes) in wells was washed, and post-incubated with NPP (**F**) or antithrombin-deficient plasma (ATDP) (**G**) in the presence of vehicle medium or Nb106 (100 µg/mL). Fluorescence from Z-GGR-AMC cleavage was measured over time (mean ± SD, n=3). Binding characterization studies of selected single-chain antibody Nb106.

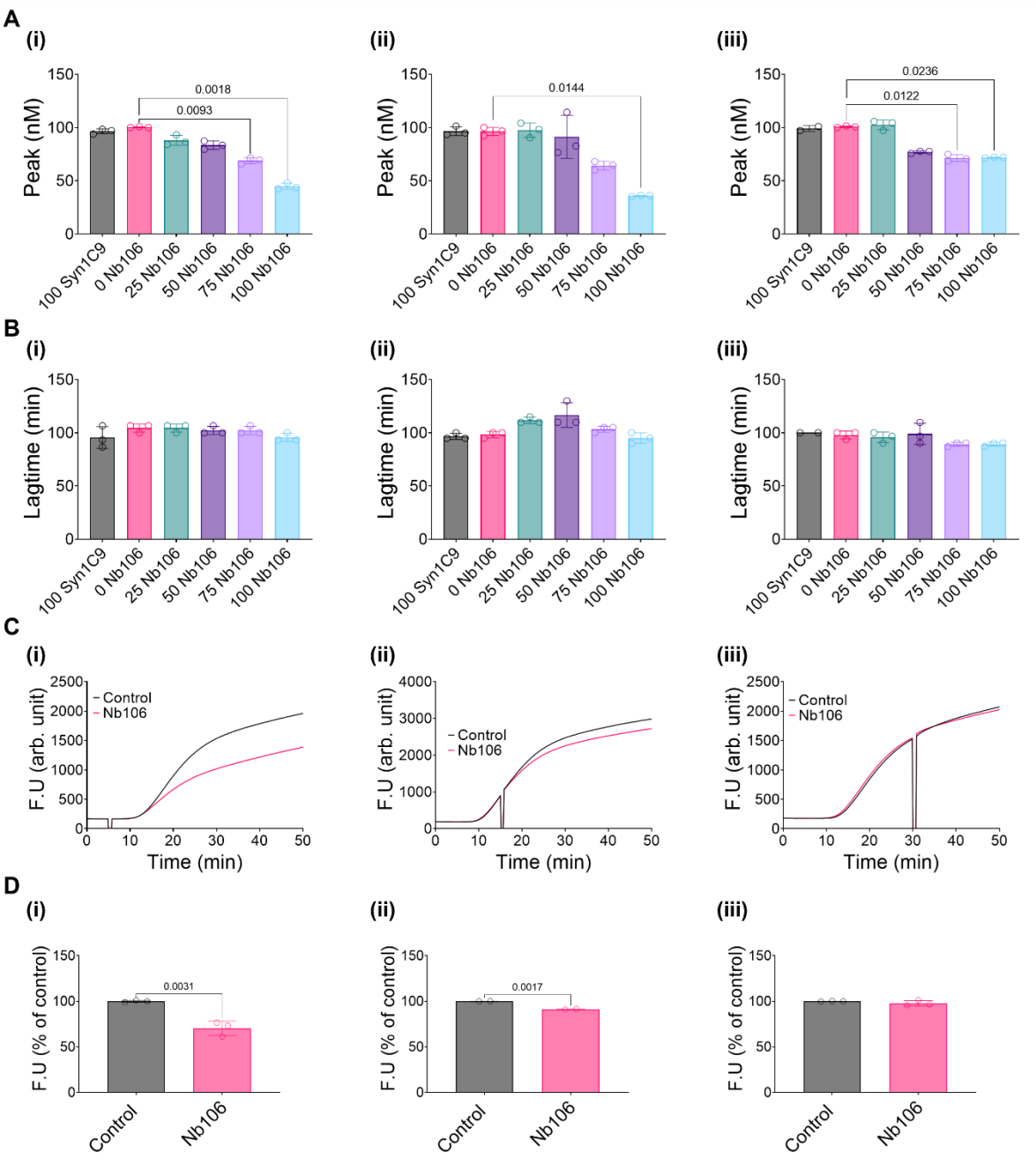

Suppl. Figure 2. Assessment of the anticoagulant potential of anti-fibrin Nb106.

(**A-B**) Parallel samples of plasma (**i**), PRP (**ii**) and whole blood (**iii**) were pre-incubated with vehicle control solution, Nb106 (25-100 µg/mL) or indifferent Nb-Syn1C9 (100 µg/mL). Coagulation was triggered with 1 pM TF, as in Figure 1. Shown are maximal thrombin levels (**A**) and lag times (**B**) relative to the control condition. Means ± SD (n=3), one-way ANOVA (non-parametric). (**C-D**) Plasma samples were triggered with 1 pM TF, and Nb106 (100 µg/mL) was added at 5 (**i**), 15 (**ii**) or 30 (**iii**) minutes. Shown are raw fluorescence curves of thrombin substrate cleavage (**C**), and normalized fluorescence values after 50 minutes (**D**). Mean ± SD (n=3), Mann-Whitney U-test. Note gradual decline of Nb106 inhibition over time. Note that Nb106 effect sizes were similar at 0.1 and 10 pM TF.

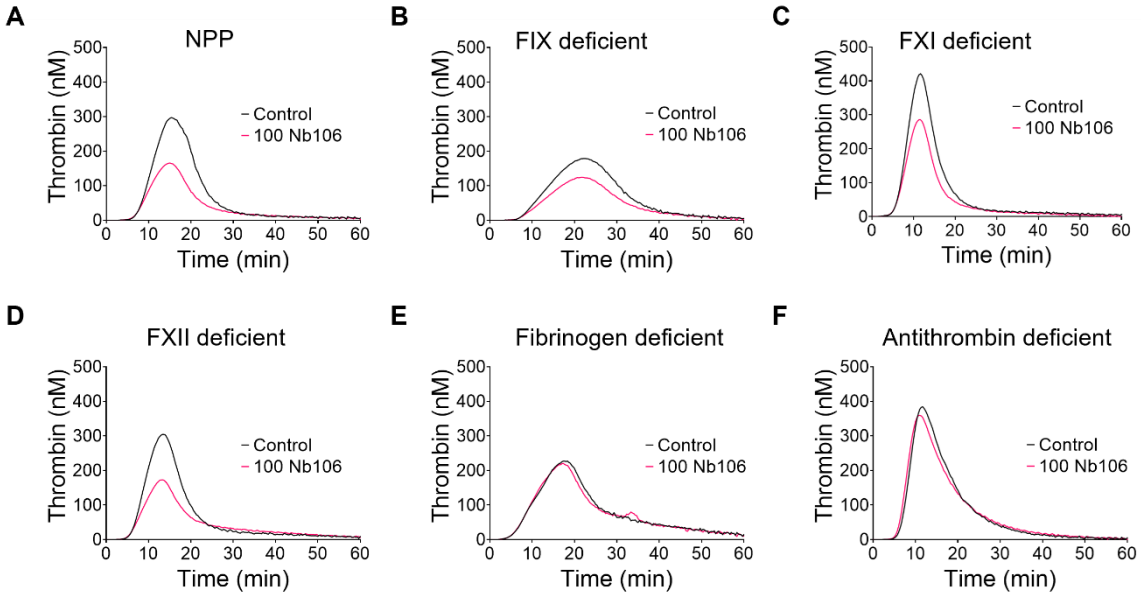

G

Plt + Plasma deficiency	Effect of Nb106 (control 100%)					
	Relative lagtime (%)	*P*	Relative peak (%)	*P*	Relative ETP (%)	*P*
None (NPP)	98 ± 2	*0.37*	56 ± 7	*0.001*	60 ± 1	*0.001*
Fibrinogen	99 ± 0.3	*0.42*	99 ± 0.3	*0.17*	98 ± 1	*0.14*
Factor IX	102 ± 2	*0.52*	69 ± 3	*<0.001*	70 ± 2	*0.001*
Factor XI	98 ± 3	*0.37*	68 ± 2	*<0.001*	69 ± 1	*<0.001*
Factor XII	101 ± 1	*0.37*	57 ± 3	*<0.001*	72 ± 3	*0.001*
Antithrombin	96 ± 3	*0.16*	95 ± 0.4	*0.08*	100 ± 1	*0.81*

Suppl. Figure 3. Thrombin-inhibiting effect of Nb106 in reconstituted PRP relying on plasma fibrinogen and antithrombin.

(**A-G**) Thrombin generation was triggered with TF using different plasma types after incubation with vehicle control solution or Nb106 (100 µg/mL). Plasma types were supplemented with platelets (2×10^8/mL) from three donors to obtain reconstituted PRP. Compared were normal pool plasma (NPP) (**A**), and plasmas deficient in factor IX (**B**), factor XI (**C**), factor XII (**D**), fibrinogen (**E**), or antithrombin (**F**). Shown are representative curves and quantified curve parameters thrombin lag time, maximum and capacity (ETP), with statistics (**G**). Mean ± SD (n=3-5), two-way ANOVA, non-parametric.

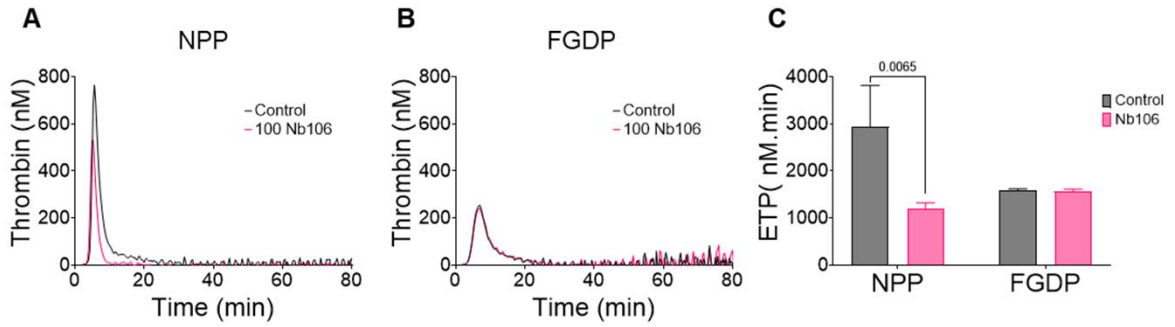

Suppl. Figure 4. Thrombin-inhibiting effect of Nb106 upon triggering with kaolin. (**A-C**) Thrombin generation was triggered in normal pool plasma (NPP) (**A**) or fibrinogen-deficient plasma (FGDP) (**B**) with $CaCl_2$/$MgCl_2$ and phospholipids plus 5 µg/mL kaolin, as in aPTT. Preincubation was with vehicle solution (control) or 100 µg/mL Nb106. (**C**) Quantification of thrombin capacity (ETP). Mean ± SD (n=3 experiments), two-way ANOVA, non-parametric).

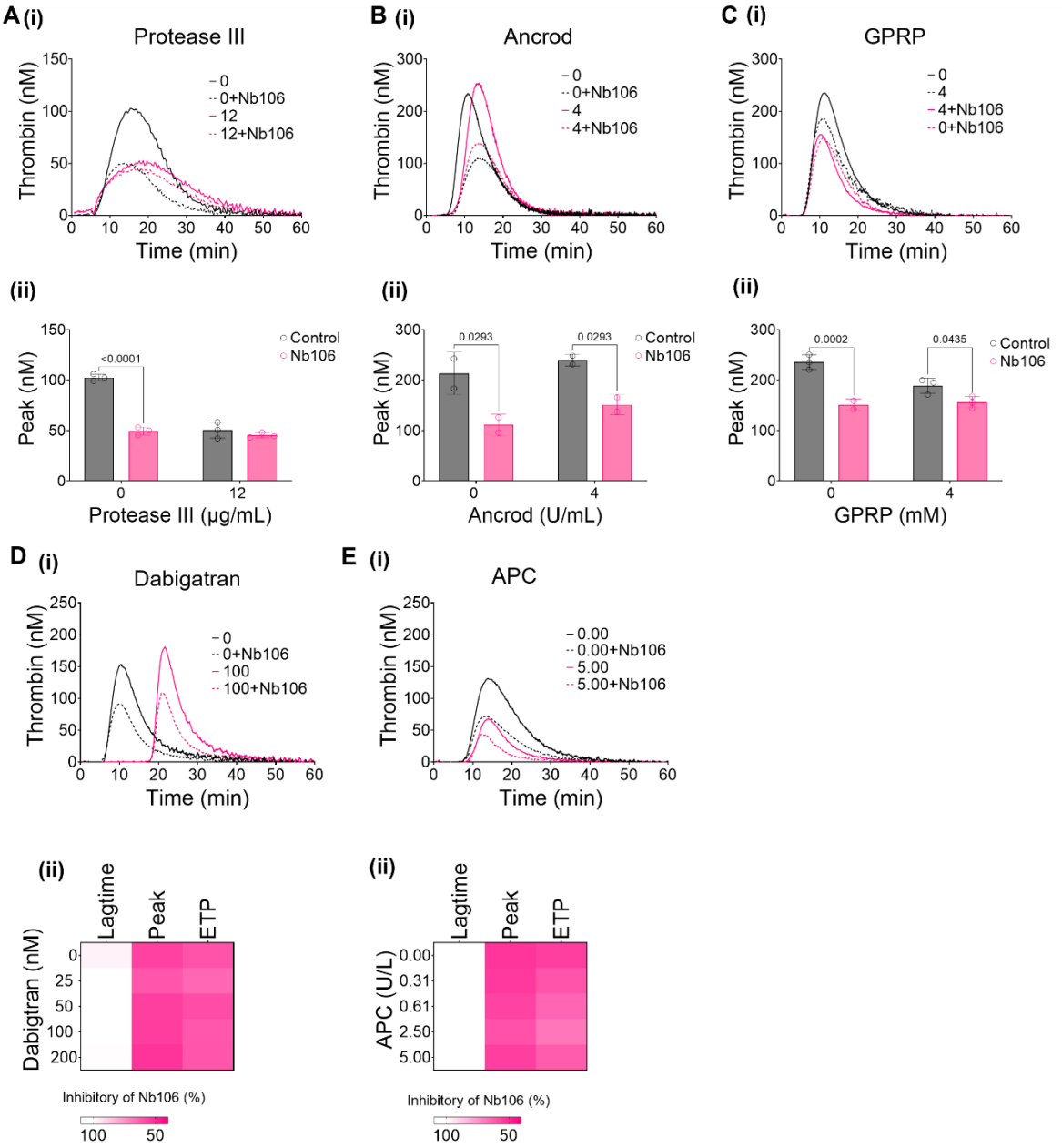

Suppl. Figure 5. Effects of fibrinogen degradation and coagulation interference on Nb106 inhibition.

(**A-C**) Normal pool plasma was preincubated with vehicle, 12 µg/mL protease III (**A**), 4 units/mL protease ancrod (**B**) or 4 mM GPRP (**C**). Coagulation was triggered with TF in the absence or presence of Nb106 (100 µg/mL), as in Figure 1. Shown are representative thrombin generation curves (**i**), and maximal thrombin levels (**ii**). Mean ± SD (n=3 experiments), two-way ANOVA (non-parametric). (**D-E**) Plasma samples were preincubated with 100 nM dabigatran (**D**) or 2.5 nM activated protein C (APC) (**E**). Representative traces of thrombin generation (**i**) and heat-mapped normalized values of curve parameters (**ii**). Mean results from triplicate experiments. Colour bar indicates inhibitory effect of Nb106 versus corresponding control condition.

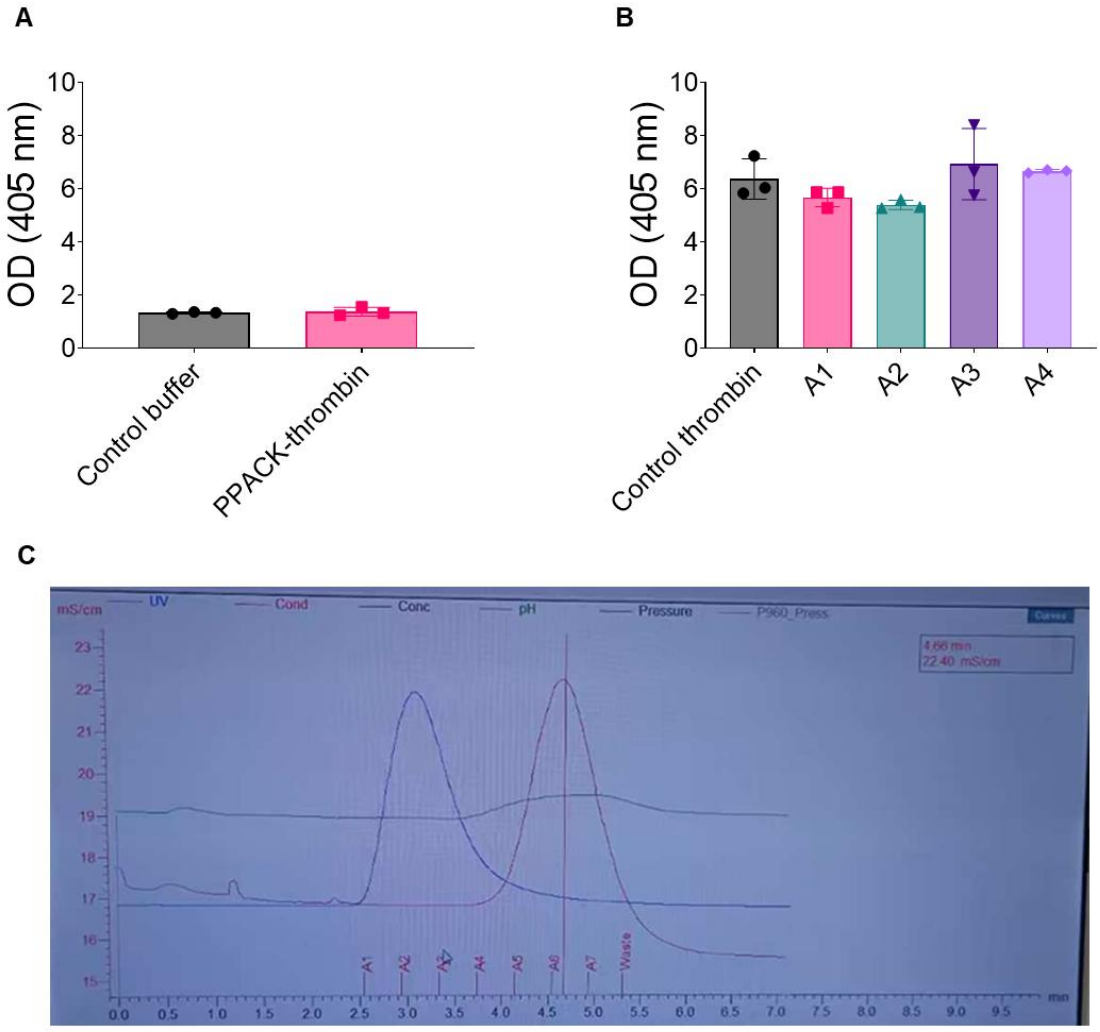

Suppl. Figure 6. Purification of PPACK–thrombin and activity testing of free thrombin and free PPACK.

(**A**) Activity testing of residual free thrombin. Thrombin activity was assessed by chromogenic substrate S2238 cleavage at 405 nm. PPACK–thrombin showed no detectable residual thrombin activity compared with control buffer. Mean ± SD (n=3 experiments), one-way ANOVA (non-parametric). (**B**) Residual free PPACK activity after desalting. Following purification on a desalting column, fractions A1–A4 were tested for free PPACK activity using chromogenic substrate S2238 at 405 nm. No residual free PPACK activity was detected in any fraction compared with control thrombin. Mean ± SD (n=3 experiments), one-way ANOVA (non-parametric). (**C**) Chromatographic profile of PPACK–thrombin purification. Representative chromatogram from desalting column purification. Fractions A1–A4 correspond to the main elution peak collected for further analysis.

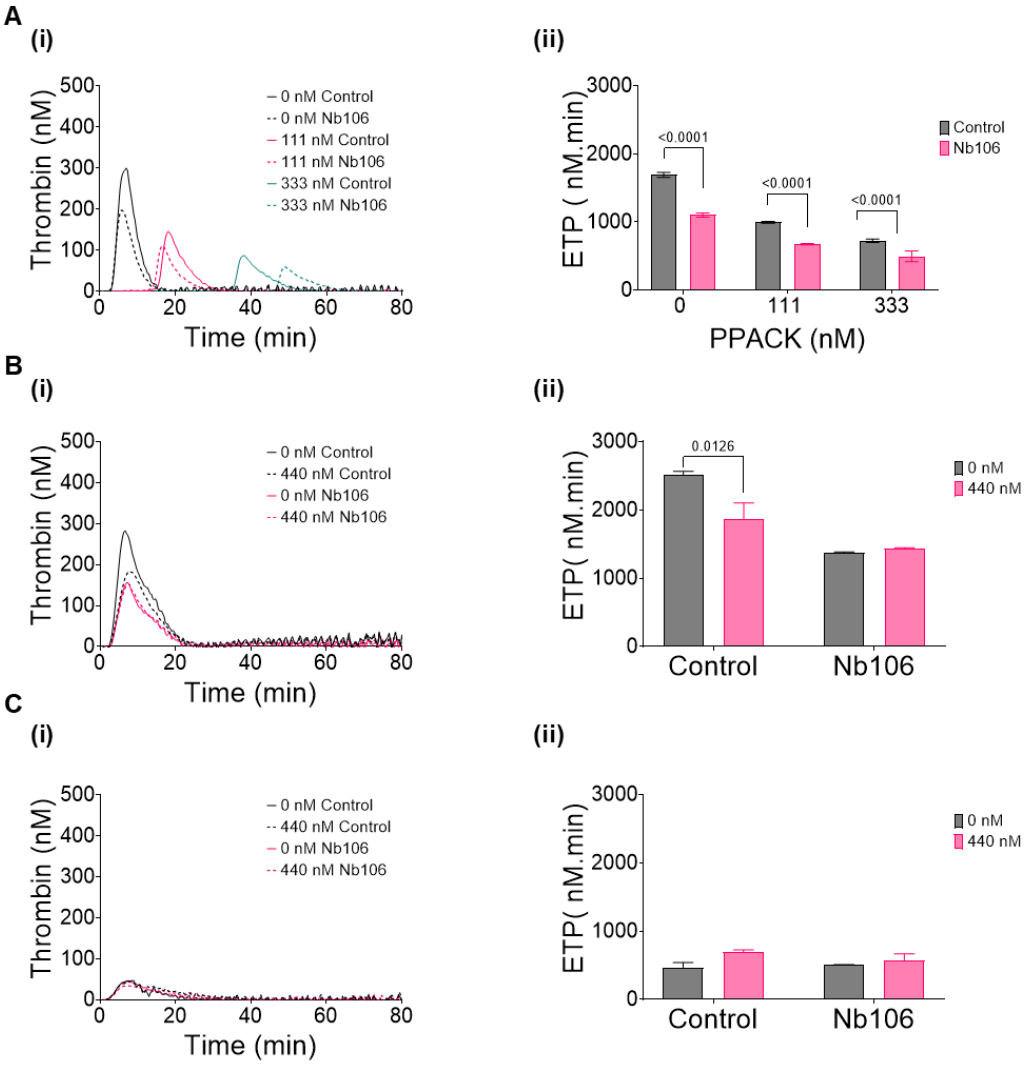

Suppl. Figure 7. Similar effects of PPACK-thrombin and Nb106 but not PPACK on thrombin generation.

(**A**) Consistent Nb106 effect on thrombin generation in the presence of PPACK. Thrombin generation in normal pool plasma was triggered as in Figure 1 with 1 pM TF in the absence or presence of Nb106 (100 µg/mL). Plasma samples were preincubated with indicated concentrations of PPACK (0, 111 and 333 nM). (**B-C**) Effects of PPACK-inactivated thrombin and Nb106 on thrombin generation. Thrombin generation in normal pool plasma (NPP) (**B**) or in fibrinogen-deficient plasma (FDP) (**C**) was triggered with 1 pM TF. Plasma samples were preincubated with vehicle (control), purified PPACK-thrombin (440 nM) and/or Nb106 (100 µg/mL). Mean ± SD (n=3 experiments), two-way ANOVA (non-parametric).

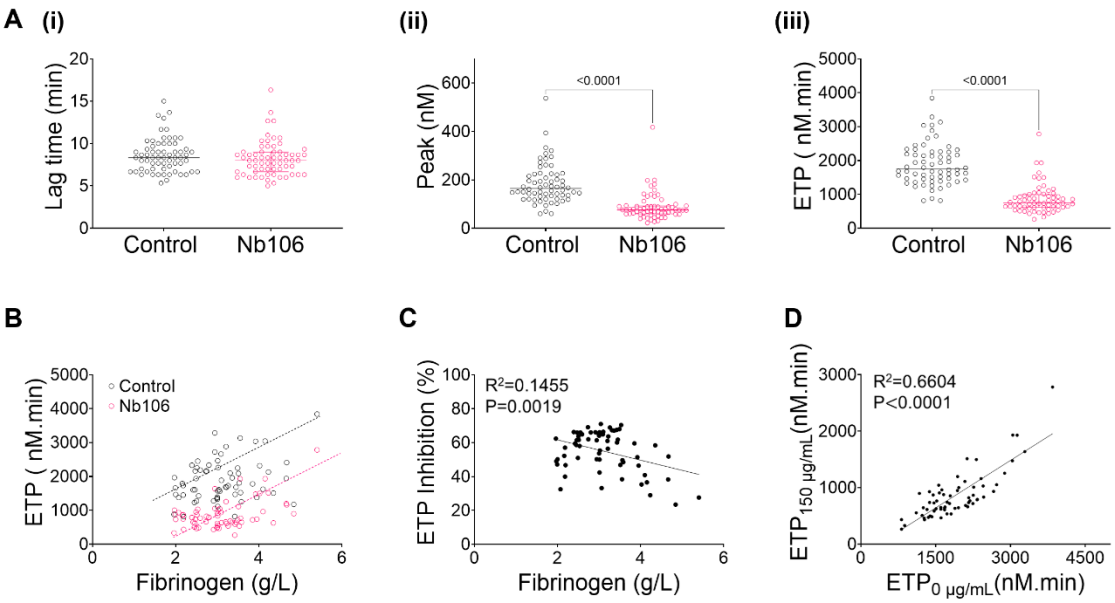

Suppl. Figure 8. Fibrin-dependent thrombin generation in cohort of healthy subjects.
Plasma samples from 64 healthy subjects were in part pre-incubated with Nb106 (150 µg/mL). TF-induced thrombin generation was assessed, as in Figure 1. (**A**) Indicated are per subject Nb106-mediated changes in thrombin lag time (**i**), maximal thrombin (**ii**) and thrombin capacity (ETP) levels (**iii**). Furthermore, (**B**) plots of plasma fibrinogen (Claus method) and thrombin capacity with(out) Nb106. Shown are conditions of control and Nb106 (n=64), p values in italic (Mann-Whitney U-test). (**C**) Effect of Nb106 on thrombin capacity, and (**D**) correlation of thrombin capacity levels with or without Nb106.

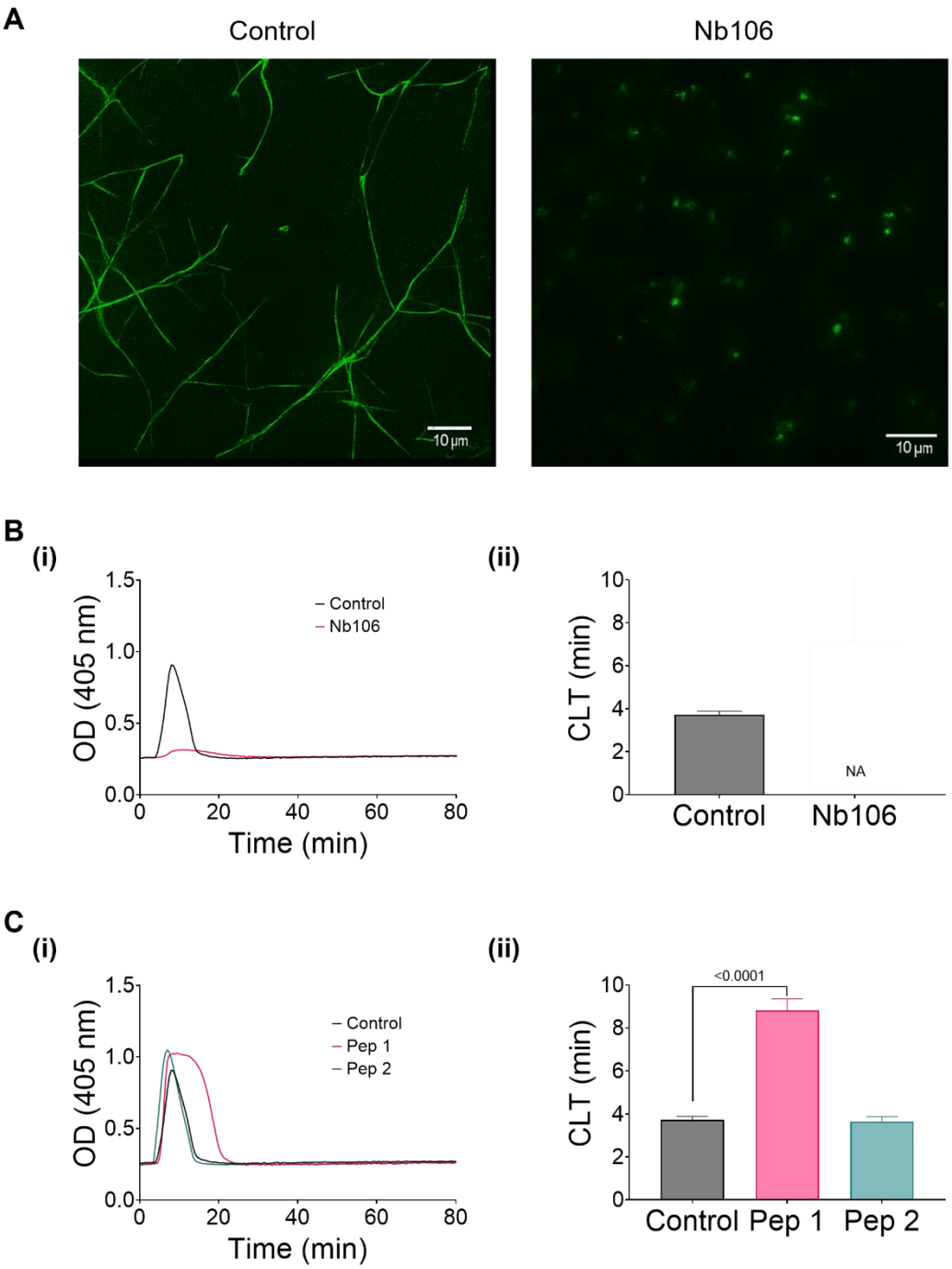

Suppl. Figure 9. Nb106 effects on clot lysis and on fibrin network formation.

(**A**) Representative confocal fluorescence microscopy images of fibrin structures from tissue-factor triggered plasmas in the absence (left) or presence (right) of Nb106 (100 µg/mL). Fibrin was formed from labeled Alexa Fluor-488 fibrinogen (green). Scale bar=10 µm. (**B-C**) Normal plasma containing tPA (3 nM) was triggered with $CaCl_2$/$MgCl_2$, phospholipids and 1 pM TF. Changes in optical density at 405 nm were followed at 37 °C to measure clot formation and subsequent lysis. (**B**) Plasma samples containing vehicle control medium or Nb106 (100 µg/mL). (**C**) Parallel samples contained Pep1 (500 µM) or Pep2 (500 µM), as indicated. Optical density traces are presentative for 3 experiments. Mean ± SD, one-way ANOVA (non-parametric).

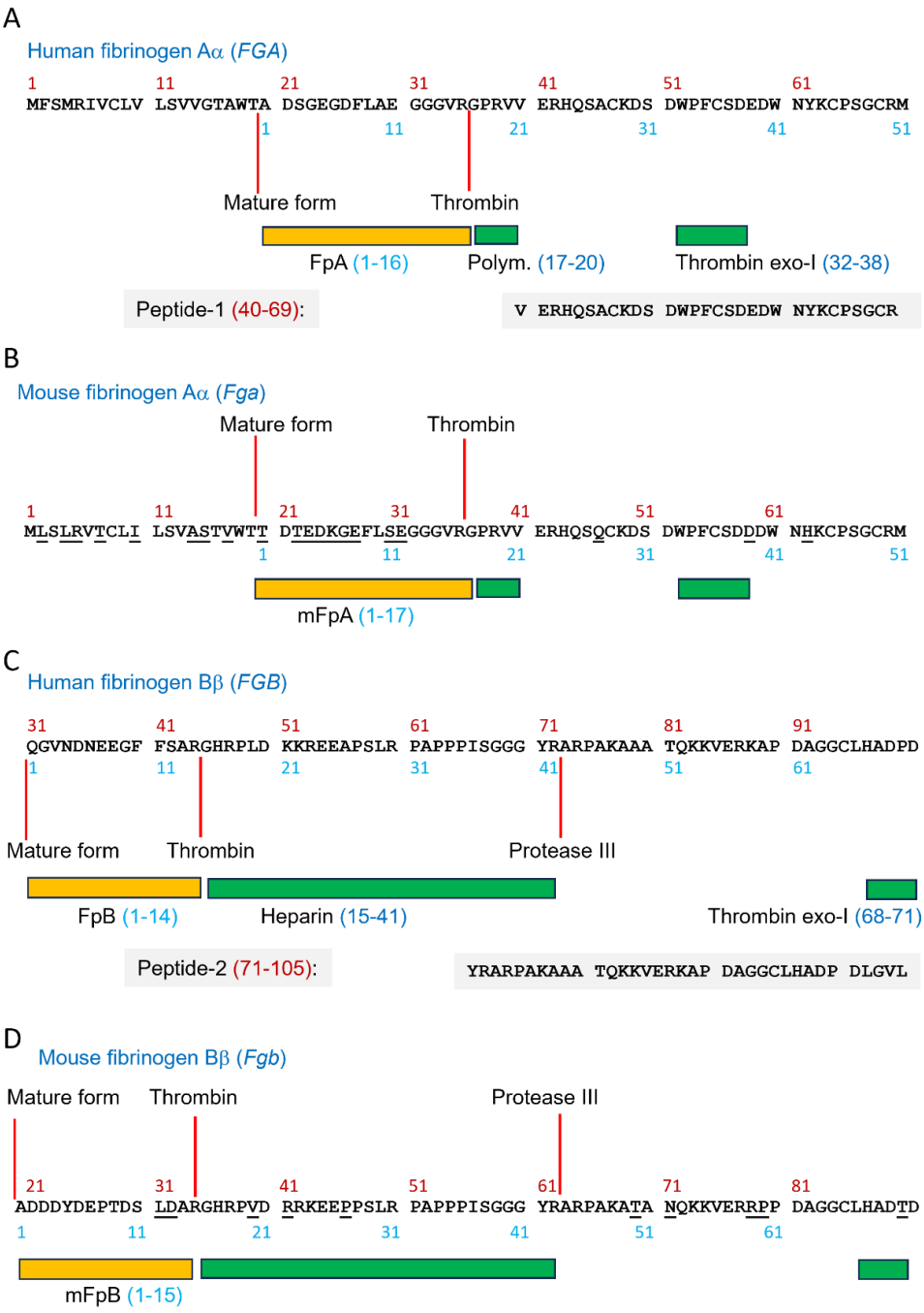

Suppl. Figure 10. Primary structure of N-terminal fibrin Aα and Bβ chains and the derived peptides.

(**A-B**) Primary amino acid sequence of human (UniProtKB P02671) and mouse (E9PV24) N-terminal parts of fibrinogen α-chains. Indicated are cleavage sites by maturation and thrombin. Numbering in red is according to corresponding transcripts, in blue according to the mature proteins. Indicated are the sequence of cleaved FpA peptide, of fibrin polymerization site and of postulated thrombin binding site via exosite-I.[22] Underlined are the non-conserved amino acid residues in the mouse protein. (**C-D**) Idem for the human (P02675) and mouse (Q8K0E8) N-terminal parts of fibrinogen β-chains. Indicated are cleavage sites by maturation, thrombin and protease III. Furthermore, sequences of cleaved FpB peptide, of heparin-platelet binding domain[27], and of postulated thrombin binding site via exosite-I.[22]

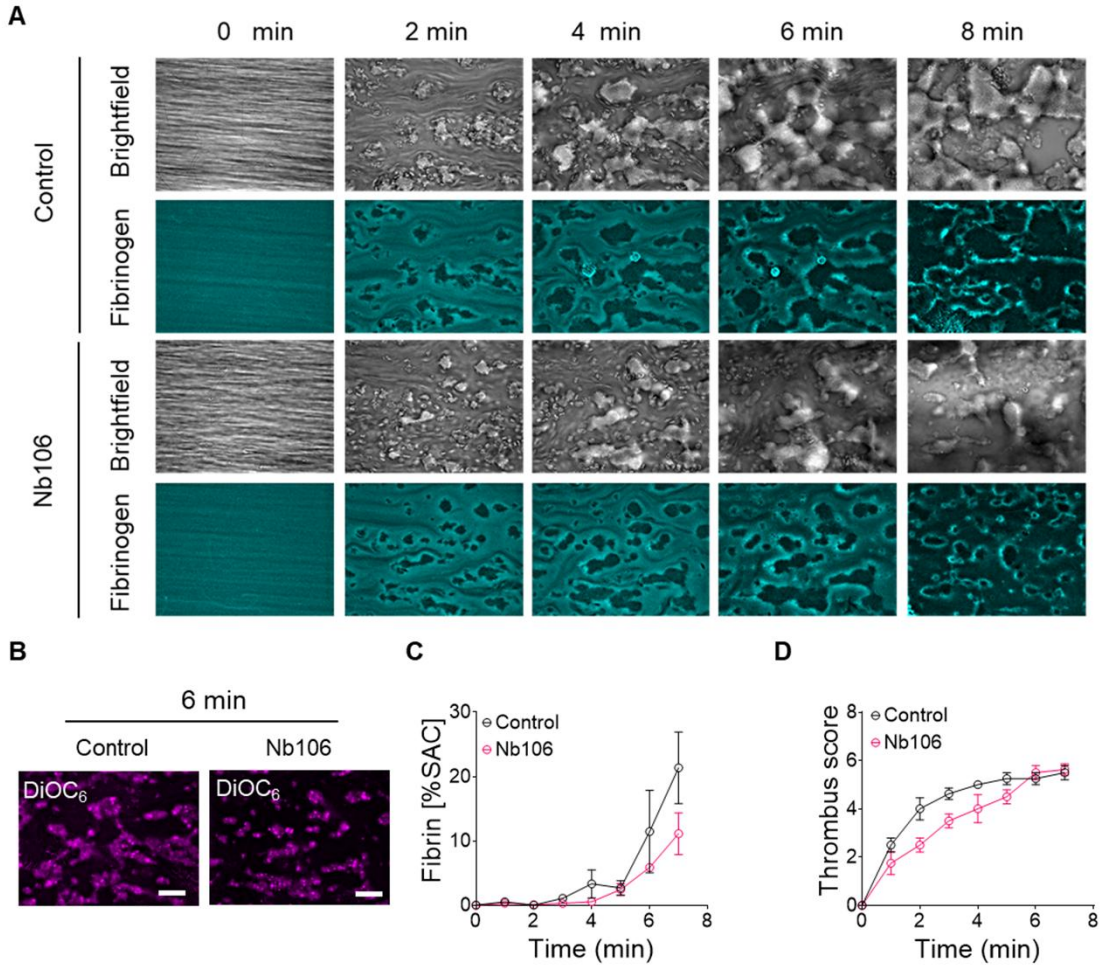

Suppl. Figure 11. Unaltered murine thrombus formation at high shear rate of 1000 s^{-1}.
(**A-B**) Citrated mouse blood was supplemented with Alexa Fluor 488-fibrinogen (green) and Alexa Fluor 647-anti-GPIX mAb (purple), with Nb106 (100 µg/mL) present as indicated. Blood samples were continuously recalcified with 1 pM TF, while perfusing over collagen-I microspots at high, arterial shear rate of 1000 s^{-1}. (**A**) Representative brightfield and fluorescence images of platelet-fibrin thrombi during flow. (**B**) Representative images of 6-minutes platelet deposition (AF647-αGPIX). Bars = 20 µm. (**C**) Quantification of fibrin surface area coverage and (**D**) thrombus score on scale 1-6 over time. Mean ± SD (n=4), two-way ANOVA. Note that fluorescence detection threshold was set above the background level of dissolved AF647-fibrinogen, to capture only increased levels of polymerized fibrin fluorescence.

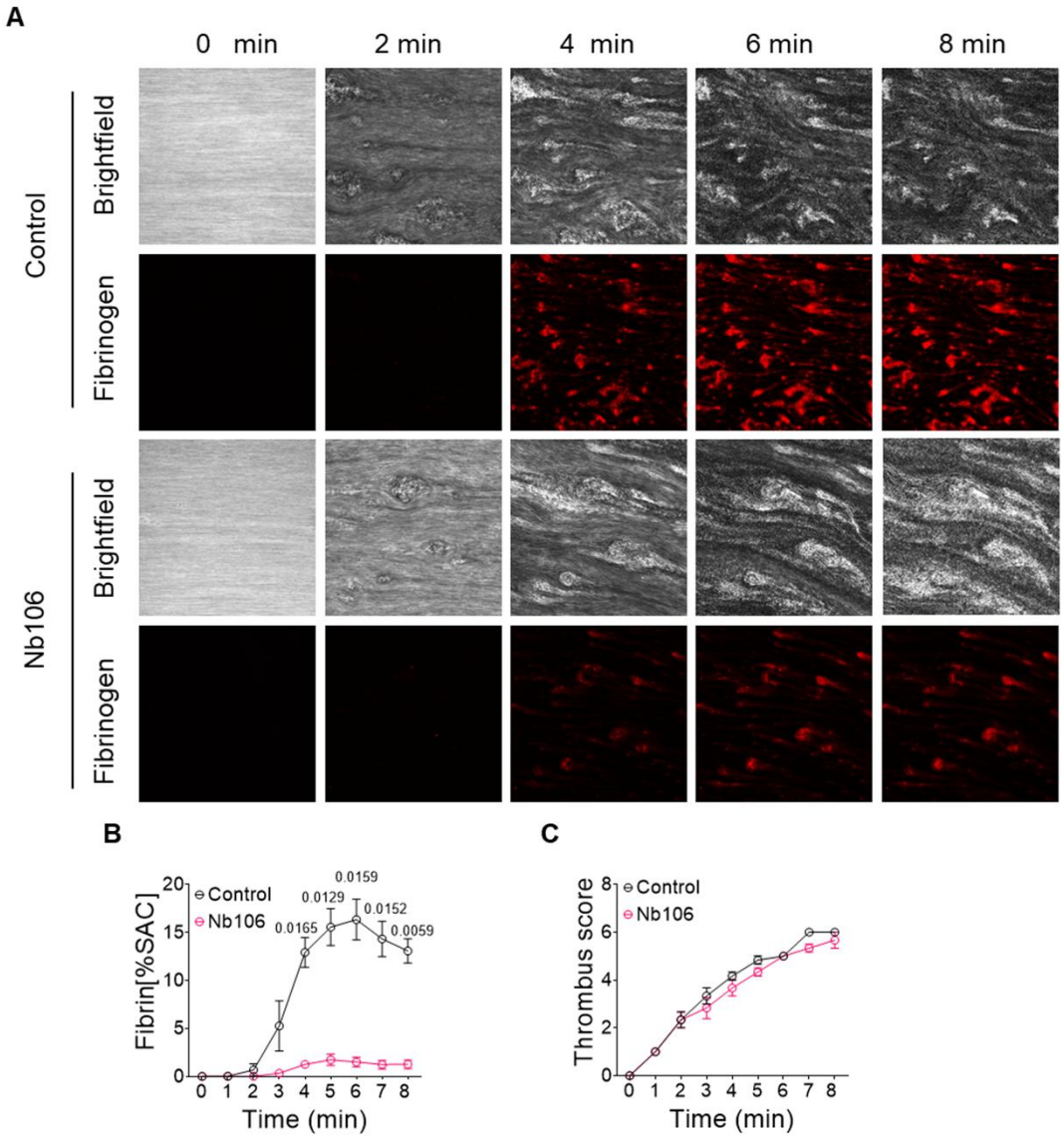

Suppl. Figure 12. Suppression by Nb106 of human thrombus formation limited to low shear rate of 200 s^{-1}.

(**A-C**) Citrated human blood samples were supplemented with Alexa Fluor 647-fibrinogen and with vehicle medium or Nb106 (100 µg/mL), as indicated. Blood perfusion was under continuous recalcification with 1 pM TF over collagen-I microspots at wall-shear rate of 200 s^{-1}.[25] (**A**) Representative brightfield and fluorescence images of fibrin-containing thrombi during flow in the absence or presence of Nb106. (**B**) Quantification of fibrin surface area coverage over time. (**C**) Quantification of thrombus score. Mean ± SD (n=4), two-way ANOVA.

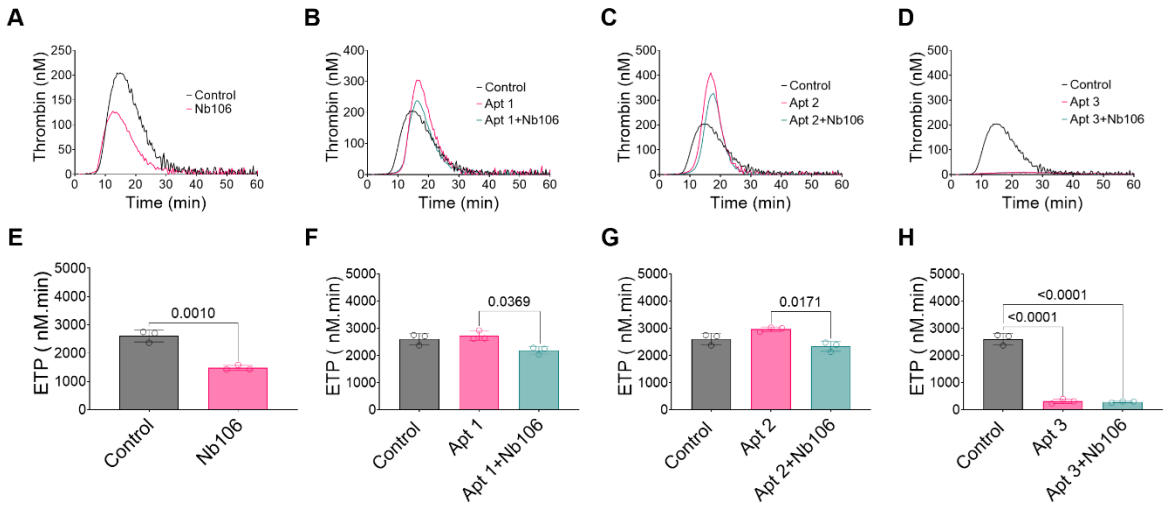

Suppl. Figure 13. Procoagulant effect of thrombin exosite-I or exosite-II inhibition.

To achieve thrombin exosite-I, exosite-II or combined exosite-I+II inhibition, plasma samples from healthy subjects were incubated with 5.3 μM Apt1, Apt2 or Apt3, respectively. TF-induced (1 pM) thrombin generation was measured in the absence or presence of Nb106 (100 μg/mL). Representative curves show effect of Nb106 alone (**A**), of Apt1 (**B**), Apt2 (**C**) or Apt3 (**D**). Furthermore , quantified maximal thrombin levels at these conditions (**E-H**). Mean ± SD (n=3).

References

1. Miszta A, Pelkmans L, Lindhout T, et al. Thrombin-dependent incorporation of von Willebrand factor into a fibrin network. *J Biol Chem*. 2014;289:35979–35986.
2. Wan J, Konings J, Yan Q, et al. A novel assay for studying the involvement of blood cells in whole blood thrombin generation. *J Thromb Haemost*. 2020;18:1291–1301.
3. Kremers RM, Kleinegris MC, Ninivaggi M, et al. Decreased prothrombin conversion and reduced thrombin inactivation explain rebalanced thrombin generation in liver cirrhosis. *PLoS One*. 2017;12:e0177020.
4. Sun S, Campello E, Zou J, et al. Crucial roles of red blood cells and platelets in whole blood thrombin generation. *Blood Adv*. 2023;7:6717–6731.
5. Macrae FL, Swieringa F, Heemskerk JW, Ariens RA. High fibrinogen γ' levels in patient plasma increase clot formation at arterial and venous shear rate. *Blood Adv*. 2021;5:3468–3477.
6. De Maat S, van Dooremalen S, de Groot PG, Maas C. A nanobody-based method for tracking factor XII activation in plasma. *Thromb Haemost*. 2013;110:458–468.
7. Wohner N, Sebastian S, Muczynski V, et al. Osteoprotegerin modulates platelet adhesion to von Willebrand factor during release from endothelial cells. *J Thromb Haemost*. 2022;20:755–766.
8. Marchi R, Vilar R, Durual S, et al. Fibrin clot properties to assess the bleeding phenotype in unrelated patients with hypodysfibrinogenemia due to novel fibrinogen mutations. *Thromb Res*. 2021;197:56–64.
9. Marchi R, Neerman-Arbez M, Gay V, et al. Comparison of different activators of coagulation by turbidity analysis of hereditary dysfibrinogenemia and controls. *Blood Coagul Fibrinolysis*. 2021;32:108–114.
10. Vanschoonbeek K, Feijge MA, van Kampen RJ, et al. Initiating and potentiating role of platelets in tissue factor-induced thrombin generation in the presence of plasma: subject-dependent variation in thrombogram characteristics. *J Thromb Haemost*. 2004;2:476–484.
11. De Laat B, Stragier H, de Laat-Kremers R, et al. Population-wide persistent hemostatic changes after vaccination with ChAdOx1-S. *Front Cardiovasc Med*. 2022;9:966028.
12. Beck S, Öftering P, Li R, et al. Platelet glycoprotein V spatio-temporally controls fibrin formation. *Nat Cardiovasc Res*. 2023;2:368–382.

13. Brouns S, van Geffen JP, Campello E, et al. Platelet-primed interactions of coagulation and anticoagulation pathways in flow-dependent thrombus formation. *Sci Rep*. 2020; 10:11910.
14. Mattheij NJ, Braun A, van Kruchten R, et al. Survival protein anoctamin-6 controls multiple platelet responses including phospholipid scrambling, swelling, and protein cleavage. *FASEB J*. 2016;30:727–737.
15. Al Dieri R, de Laat B, Hemker HC. Thrombin generation: what have we learned? *Blood Rev*. 2012;26:197–203.
16. Hemker HC, Giesen P, Al Dieri R, et al. Calibrated automated thrombin generation measurement in clotting plasma. *Pathophysiol Haemost Thromb*. 2003;33:4–15.
17. Kessels H, Willems G, Hemker HC. Analysis of thrombin generation in plasma. *Comput Biol Med*. 1994;24:277–288.
18. de Laat-Kremers RMW, Yan Q, Ninivaggi M, de Maat M, de Laat B. Deciphering the coagulation profile through the dynamics of thrombin activity. *Sci Rep*. 2020;10:12544.
19. Longstaff C. Measuring fibrinolysis: from research to routine diagnostic assays. *J Thromb Haemost*. 2018;16:652–662.
20. Campello E, Marobin M, Barbot M, et al. The haemostatic system in acromegaly: a single-centre case-control study. *J Endocrinol Invest*. 2020;43:1009–1018.
21. Aleman MM, Byrnes JR, Wang JG, et al. Factor XIII activity mediates red blood cell retention in venous thrombi. *J Clin Invest*. 2014;124:3590–3600.
22. Pechik I, Madrazo J, Mosesson MW, Hernandez I, Gilliland GL, Medved L. Crystal structure of the complex between thrombin and the central E region of fibrin. *Proc Natl Acad Sci USA*. 2004;101:2718–2723.
23. Willems RA, Konings J, Huskens D, et al. Altered whole blood thrombin generation and hyperresponsive platelets in patients with pancreatic cancer. *J Thromb Haemost*. 2024;22:1132–1144.
24. De Witt SM, Swieringa F, Cavill R, et al. Identification of platelet function defects by multi-parameter assessment of thrombus formation. *Nat Commun*. 2014;5:4257.
25. Navarro S, Stegner D, Nieswandt B, Heemskerk JW, Kuijpers ME. Temporal roles of platelet and coagulation pathways in collagen and tissue factor induced thrombus formation. *Int J Mol Sci*. 2021;23:358.

26. Herfs L, Swieringa F, Jooss N, et al. Multiparameter microfluidics assay of thrombus formation reveals increased sensitivity to contraction and antiplatelet agents at physiological temperature. *Thromb Res*. 2021;203:46–56.
27. Mosesson MW. Fibrinogen and fibrin structure and functions. *J Thromb Haemost*. 2005;3:1894–1904.